Limit Analysis of the Great Hall of Trajan's Markets in Rome Using Equilibrium Methods

by

Miryam Y. Dreyfuss

Bachelor of Science in Physics
New York University, 2010

Bachelor of Engineering in Mechanical Engineering
Stevens Institute of Technology, 2010

Submitted to the Department of Civil and Environmental Engineering
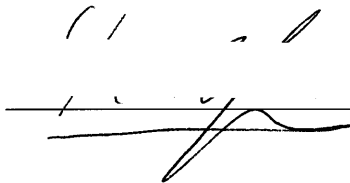in partial fulfillment of the requirements for the degree of

MASTER OF ENGINEERING IN CIVIL AND ENVIRONMENTAL ENGINEERING
at the
MASSACHUSETTS INSTITUTE OF TECHNOLOGY
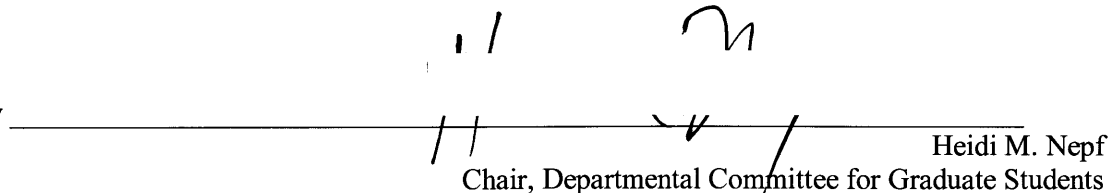
June 2011
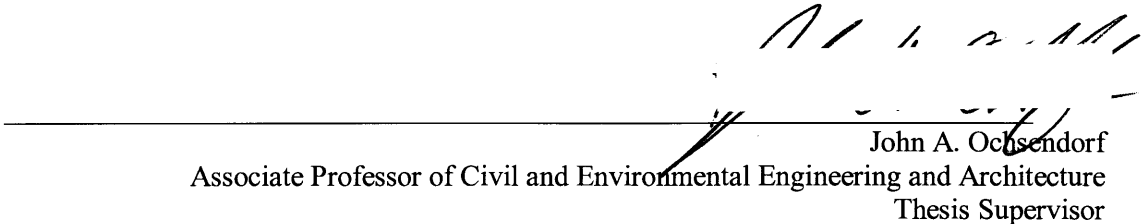
Signature of Author _____
Department of Civil and Environmental Engineering
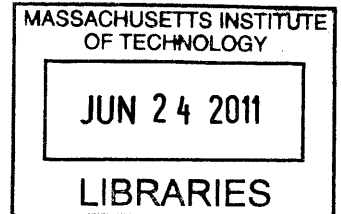May 18, 2011

Certified by _____
John A. Ochsendorf
Associate Professor of Civil and Environmental Engineering and Architecture
Thesis Supervisor

Accepted by _____
Heidi M. Nepf
Chair, Departmental Committee for Graduate Students

Limit Analysis of the Great Hall of Trajan's Markets in Rome Using Equilibrium Methods

by

Miryam Y. Dreyfuss

Submitted to the Department of Civil and Environmental Engineering on May 18, 2011 in Partial Fulfillment of the Requirements for the Degree of Master of Engineering in Civil and Environmental Engineering

Abstract

This paper studies the Great Hall of Trajan's Markets in Rome using equilibrium analysis to determine the limits of stability of its main vault under gravity loading. In particular, the capacities of three structural components were analyzed individually and as one system to compare the difference in stability limits. Recent studies of the hall that used Finite Element Methods predicted high tensile stresses in the structure, suggesting that there was a danger of further damage and potential collapse under seismic loads. This led to the installation of steel reinforcement systems within the vault and supporting structure. The objective of this thesis is to show that equilibrium methods are able to give an accurate sense of the viable states of the structure, and generally, that equilibrium methods are a more appropriate technique for analyzing highly indeterminate historic masonry structures.

The results show that the range of horizontal thrust values increases dramatically when the supporting structures (lateral arch and buttress) are included. Hence, the supporting structures are critical to the stability of the vault under static loading. Furthermore, sliding between the travertine blocks is not a consideration under static loading of the vault.

Thesis Advisor: John Ochsendorf

Title: Associate Professor of Civil and Environmental Engineering and Architecture

Acknowledgements

I would like to thank my thesis advisor, John Ochsendorf, for inspiring my interest in historic structures that led this thesis. I am grateful for all his time, help and advice this semester. Special thanks to Philip Brune for his help and providing me with his beautiful Rhino model. This thesis would have been infinitely more difficult without his generosity. In addition, I would like to thank Lynne Lancaster for allowing me to reproduce her exceptionally well-written explanation on graphic statics as an appendix in this thesis. Thanks to Jennifer Zessin who was always willing to help and was instrumental in the final stages of this paper.

Special thanks to Professor Connor and Simon Laflamme, who were crucial to the M.Eng. experience in the academic, advisory and Parisian aspects of the year. Both always had their doors open to me and other students whenever we needed anything, and I may not have survived the year without their help. Thanks also to Lauren McLean who was our mother in our home away from home.

I would like to thank my parents, who have supported me in every respect throughout my whole life. Nothing I have achieved would have been possible without them. Thank you and I love you.

Last but not least, thanks to the M.Engers who made this the best year ever. This year wouldn't have been the same without your friendship and constant distractions. I am especially grateful to my Calculator Robot. Matt's pretty cool too.

Table of Contents

1 Introduction

Trajan's Markets were built between the years 98 and 117 BCE on the Quirinal Hill in Rome. The Great Hall, or Aula Grande, occupies the north-western corner of the markets and is the most structurally elaborate aspect of the complex (Lancaster, 2005). Built by Apollodoro of Damascus, architect and engineer to the Emperor Trajan, the hall is the oldest surviving example of a cross-vault made entirely of Roman pozzolanic concrete (Perucchio, et al., 2008). The hall is approximately rectangular, 36 meters long by 8.5 meters wide, and is covered by a vault comprising six adjoining cross-vaults.

(a)   **(b)**
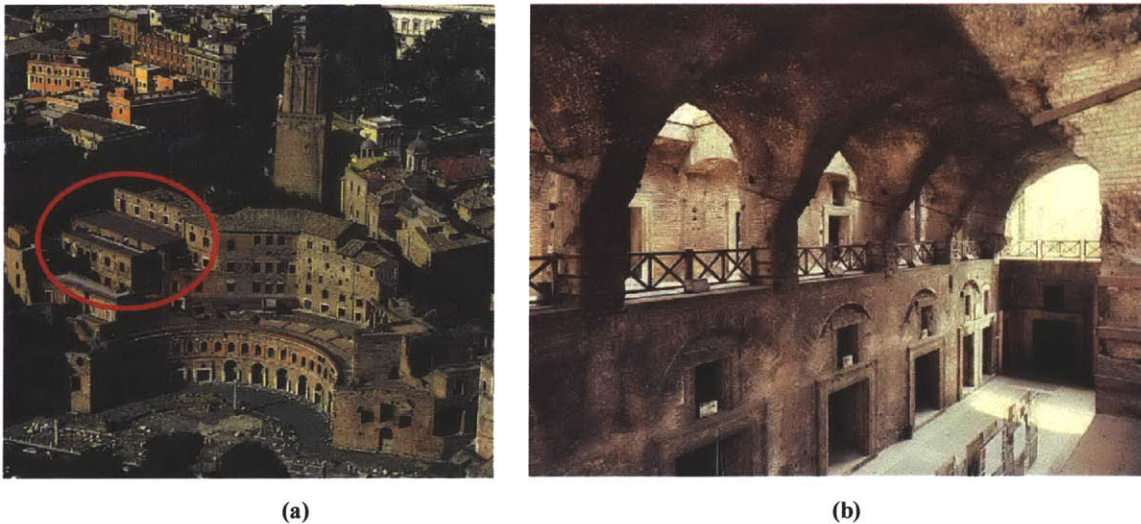
Figure 1.1 (a) Aerial view of Trajan's Markets with the Great Hall highlighted. (b) Interior of the Great Hall. (Source: http://www.fransite.net/).

The building has had a colorful history, undergoing several structural makeovers and suffering through two millennia of weather and earthquakes. These have taken a toll on the hall and damage in many locations has prompted studies by art historians, archeologists and, most recently, engineers. These analyses have led to cosmetic and structural renovations throughout the twentieth century. In the 1920's, the hall underwent a renovation to restore the original Roman features, and a seismic upgrade was introduced in 2004 (Ungaro, et al., 2008).

7

The work carried out on the hall raises many questions about the treatment of historic buildings as a structure that has been standing for hundreds, or in this case, thousands of years, should receive very careful attention. With this in mind, it is critical to fully understand the behavior of a structure before making alterations, as it is possible to cause more damage than good. Naturally, this is an extremely difficult task as such buildings are highly indeterminate structures, the materials are often not well understood and it is not always known what the structure looked like originally or how it was loaded during its service history.

Many previous attempts to model the structural behavior of historic masonry have made use of the Finite Element Method (FEM) to model the materials as elastic continua and to plot stress fields within the material. Although FEM is a very powerful tool, it is not always the one most appropriate for a given application. In certain instances more fundamental techniques, such as the equilibrium analysis employed in this paper, can provide a clearer insight into the behavior of a structure. This is especially true of historic masonry structures which typically fail due to instability rather than material weakness(Heyman, 1995). Some of the techniques previously used to analyze the hall as well as the structural interventions that followed are presented below.

This paper makes use of equilibrium methods to attempt to determine the limit states of the Great Hall of Trajan's Markets under its own weight to hone in on the possible range of solutions of the building's stability. Specifically, the role of the lateral arch and outer buttress are studied to gain some insight into the workings of the supporting structures of the hall that have contributed to the long life of the building to date. Results are compared to those obtained through FEM analysis in previous studies as a means of evaluating different methods for the particular application of historic structures. The objectives of this thesis can be summarized as follows:

- Find the limits of stability for main vault
- Determine the utility of the lateral arch and buttress in the stability of the vault
- Show that equilibrium analysis is a useful tool for the analysis of historic masonry structures

2 Background

2.1 Structural Layout and Materials

The Great Hall was an imperial public space flanked on either side by a three-level supporting structure (
Figure 2.1c). The hall is nearly rectangular in plan, 36 meters long by approximately 8.5 meters wide and 11 meters from the main floor to the vault intrados(Brune, 2010). The main floor is lined with several barrel-vaulted rooms that open into the aula. On the level above, a passageway runs longitudinally along the length of the main vault on each side, separating it from more vaulted rooms. The vault is connected to the outer structure by lateral arches that occur in line with the fourteen piers on which the vault is supported. What is thought to be the original layout of the Great Hall and its dimensions are shown in Figure 5.2.
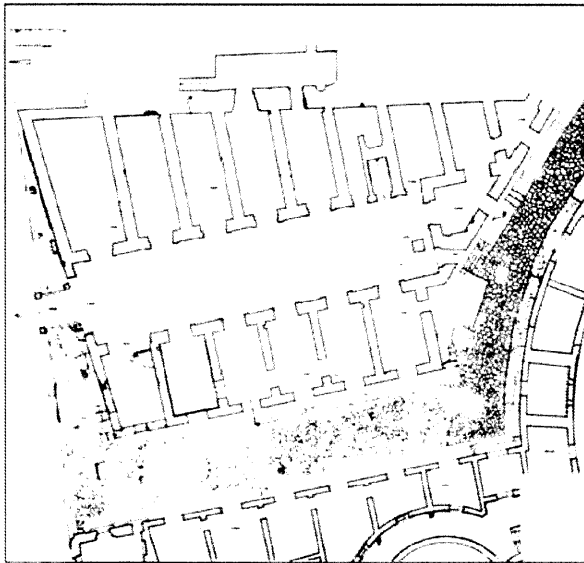
(a) Plan view of lower level of the Aula Grande
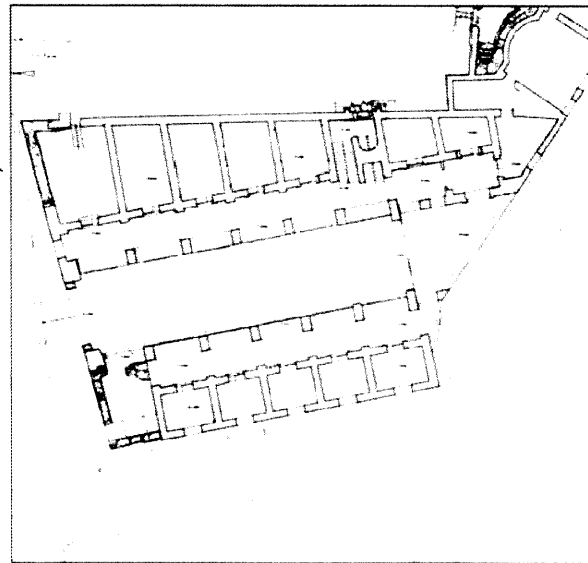
(b) Plan view of upper level of the Aula Grande
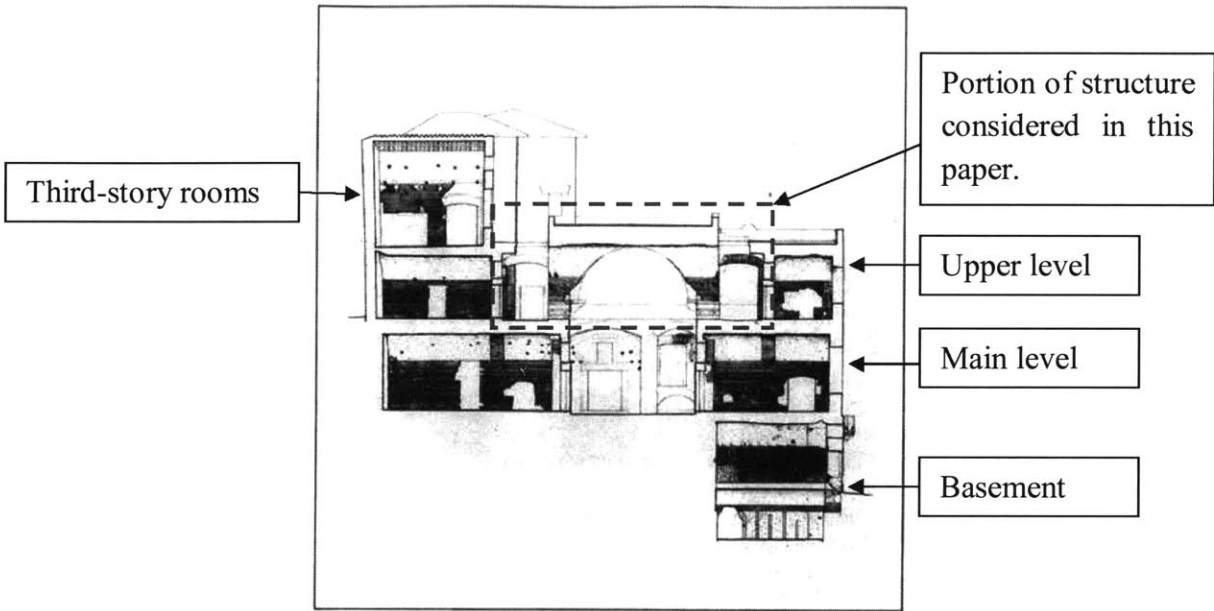
(c) Lateral section of the Great Hall.
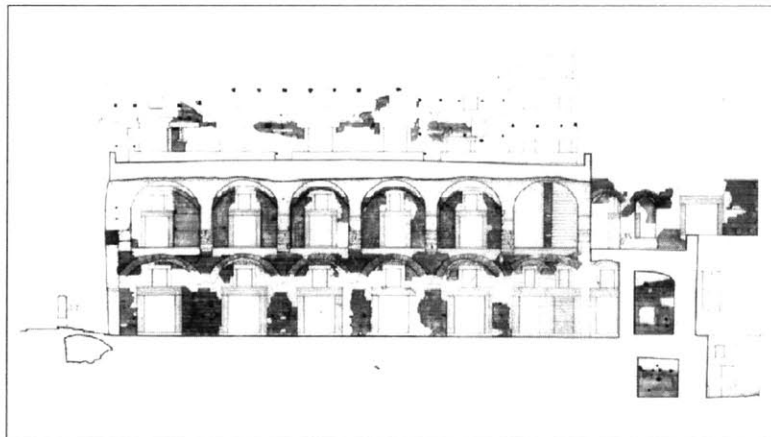
(d) Longitudinal elevation of the Great Hall.

Figure 2.1 (a) Plan view of lower level for the Aula Grande. (b) Plan view of upper level of the Aula Grande. (c) Lateral section of the hall. (d) Longitudinal elevation of the hall (Bianchini, 1991).

The vault is actually made up of six masonry cross vaults that originally sprang from corbels on fourteen travertine piers (Figure 5.2). These piers consist of two separate sections: a lower part made of a travertine ashlar block and an upper corbel (only one of which remains today, shown in Figure 2.2). The vault has a flat extrados constructed of *tufo giallo della via Tiberina*, a yellow tuff from the Sabatini district near Rome that was used for vaulting due to its lightweight properties beginning around 70 B.C.E. The vaults that cover the side rooms and passageways are

made of a combination of crushed brick and *tufo lionato*, a heavier tuff quarried from the Colli Albani district (Lancaster, 2005).

2.1.1 Clamps
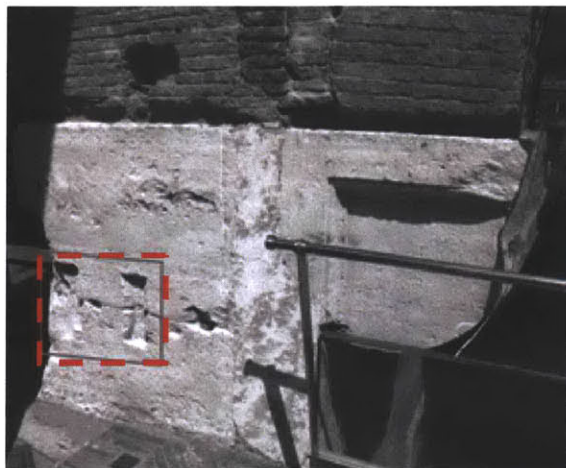
Figure 2.2 Photograph of the only remaining travertine corbel. The square shows the impressions left by butterfly clamps (Brune, 2010).

On each of the piers there are five impressions where there were once clamps that tied the upper corbel to the prismatic travertine block underneath. Such clamps came into use in Rome when travertine became a more widely used construction material towards the end of the second century B.C.E. (Lancaster, 2005). They were often used during construction and iron elements were sometimes used to counter lateral thrusts exerted by vaulted structures, although their exact purpose is not known. It is possible that they were used to prevent sliding between the blocks, which is extremely important in the overall stability of the structure. Sliding concerns are included in more detail in § 3 and 5.4.

2.2 Monument History

2.2.1 Conversion into the convent of St. Catherine of Siena, 16th Century

The Great Hall has undergone several alterations in its 2000-year history. The original layout of the hall has been reconstructed through old paintings and sketches from the fourteenth and sixteenth centuries (Ungaro, et al., 2008). Through these works, it is thought that the cross-vaults were initially divided by transverse ribs that sprang from the corbels (Figure 2.3). These were removed during the first major renovation that occurred in the sixteenth century, when the hall

was converted into the convent of St. Catherine of Siena (up to this point, the hall was in continuous use, so no major changes were made). The hall was divided in half, and the corbels of the piers were removed (except at the southern end) to make room for the new floor. Material was removed around the piers to reshape the intrados of the vault and the side corridors were covered by a vault to create interior spaces (Ungaro, et al., 2008). An oculus, which was not a part of the original Roman construction but existed by the time of the new convent, was adapted as an air and light intake for the new upstairs space (Croci, et al., 2008).

Figure 2.3 Reconstruction of the interior of the Great Hall with the transversal ribs (Bianchini, 1991).

2.2.2 Construction during the 20th Century

In the 1920's and 30's, the hall underwent reconstruction to return it to its supposed original Roman appearance (Figure 2.3). Under the direction of Corrado Ricci, the changes made by the convent were removed including the second floor, the corridor coverings, and the oculus was closed up. Due to several large and visible cracks, metallic ties were inserted in many locations in an attempt to reduce their worsening. Such ties were placed in the vault springing, throughout the new concrete layer above the Roman pavement, and through the pillars via metallic rings (Ungaro, et al., 2008). The intrados of the vault was plastered over to cover the appearance of the cracks.

12

Figure 2.4. Restoration of the Great Hall during the 1930's (Bianchini, 2010).

In 2000, the pillars were strengthened further by removing the metallic rings from the previous renovation and inserting stainless steel bars through the widths of the pillars (Ungaro, et al., 2008).

2.2.3 Seismic Upgrade, 2004

In 2004, major seismic upgrades were made to the structure. Visual inspection and linear elastic modeling (described in § 3.1) carried out by Giorgio Croci led to conclusions that the structure was weak and required reinforcement for protection against seismic excitation. Croci's philosophy was to address the alterations on a more global scale, with the knowledge that interventions on too local a level may change the overall behavior of the structure, while also leading to higher stress concentrations. These, in turn, could lead to even greater local damage (Croci, et al., 2008). To that end, several solutions were applied to 'improve' the structure's seismic behavior based on a Finite Element Analysis (FEA) carried out to identify the behavior of the structure under seismic loading.

In the lateral direction, horizontal ties were inserted in order to improve the shear strength in the North-South direction (Figure 2.5). In the event of accelerations in this plane, the supporting structures to the North and South of the hall would displace more uniformly, working together to increase the stiffness of the overall structure, and prevent them from moving out-of-phase.
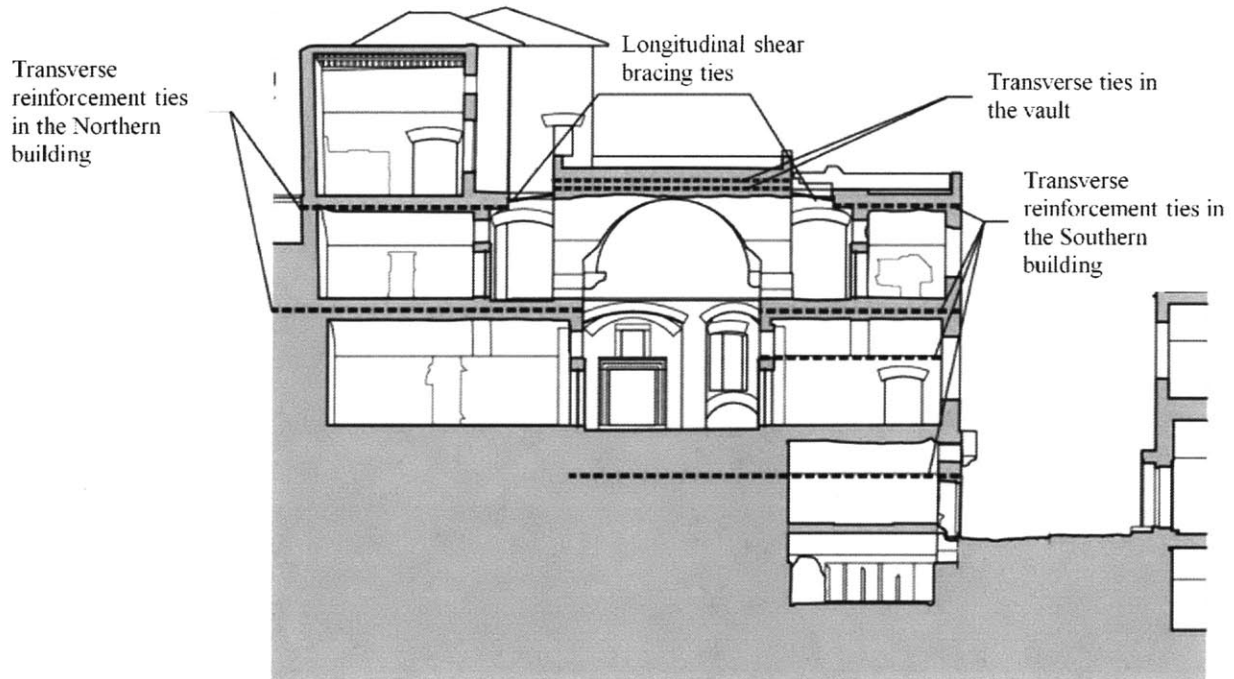
Figure 2.5 Placement of reinforcement in lateral direction (Croci, et al., 2008).

For longitudinal reinforcement, stainless steel cross-bracing was inserted horizontally in spaces at the level of the main vault. The system was designed to transfer the majority of the longitudinal seismic forces to the two buildings that laterally support the Great Hall in order to reduce the risk of overturning of the pillars, which the finite element models showed to have tensile stresses (Croci, et al., 2008). Croci did not attempt a collapse analysis, and did not demonstrate that the vault would fail in an earthquake. Rather, he predicted tensile stresses under static loading (gravity only) that would lead to failure under seismic loads. His methods are described in § 3.1.

14

2.2.4 Present State of the Hall

Figure 2.6 shows the crack pattern that has caused so much concern in recent decades. The longitudinal crack along the vault intrados is deep and runs the length of the hall. In addition, there is cracking near the supporting piers in the lateral direction. These cracks were already documented during the 1930's and led to metal ties being inserted in the material and plaster being applied to the entire intrados.
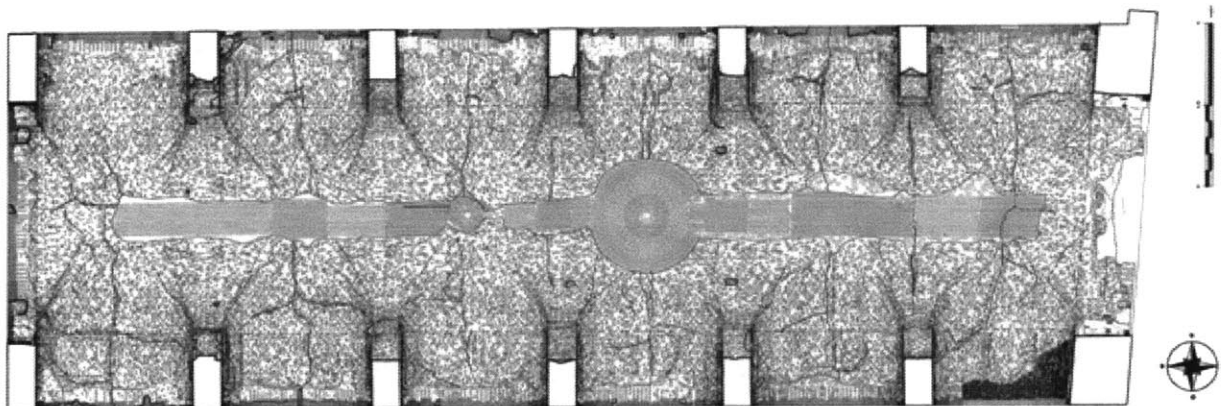
Figure 2.6 Crack pattern seen in intrados of the main vault, showing the large longitudinal crack and smaller cracks around the supports (Brune, 2010).

In 2004, the plaster was removed and the cracks were surveyed and documented (Ungaro, et al., 2008). New reinforcement schemes were implemented by Croci to prevent the cracking from getting worse or causing eventual failure during a seismic event. However, the crack pattern is typical for a cross-vault as first identified by Sabouret (1924), cited in Heyman (1995). This suggests that many of the cracks are more than 1,000 years old and do not necessarily imply that the vault is in danger of collapse.

3 Previous Analyses of the Great Hall

There have been few structural studies carried out of the Aula Grande of Trajan's Markets. Three key studies that attempt a technical analysis and are discussed in this paper are those of Ungaro et al. (2008), Croci et al. (2008) and Brune (2010). Croci and Brune make use of the Finite Element Method (FEM) to estimate the stresses occurring throughout the structure. In the Finite Element Method, it is assumed that the material is an elastic continuum, and the concrete of the hall is modeled as a linear isotropic material (although concrete is anisotropic heterogeneous), which is considered valid by Brune as long as stresses do not exceed the strength of the material (Brune, 2010). The analyses raise several questions about the nature of the structure, and indeed about the methods used for the study of masonry structures.

3.1 Seismic Analysis

One major analysis by Giorgio Croci was carried out for the design of the seismic upgrade that occurred in 2004. He carried out visual and FEM studies that led to conclusions that the Aula Grande was weak in several directions, and therefore, susceptible to collapse during a seismic event. Crack patterns suggested that the building south of the hall may have been weak with a tendency towards detachment, and required strengthening if it was to continue supporting the hall laterally (lateral section shown in Figure 2.1c). Based on a linear static analysis, Croci stated that there was little structural resistance to a possible seismic event in the longitudinal direction, as the pillars' and lateral arches' planes of stiffness are in the orthogonal direction. He infers that the overall weakness of the hall was probably due to the changes made by the works carried out in the sixteenth and early twentieth centuries (Croci, et al., 2008). In addition, he speculates that the weaknesses in both the longitudinal and lateral directions are also partly due to four major earthquakes that have occurred during the structure's lifetime. A finite element analysis confirmed tensile stresses in similar locations to where cracking was found. The finite element model was subjected to a ground acceleration and the stresses in the structure were predicted to be greater than the material strength of the concrete (Figure 3.1).
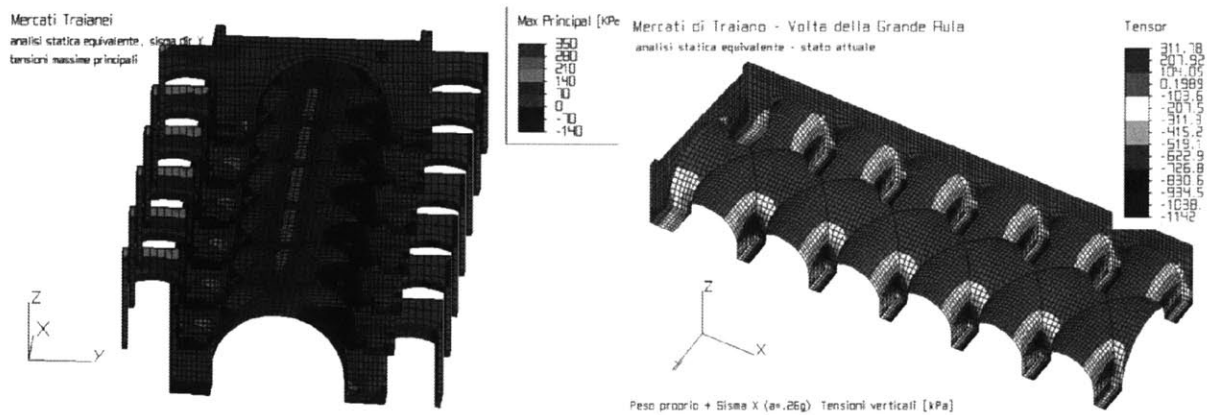
Figure 3.1. FEM results of static case (right) and with applied ground acceleration (Croci, et al., 2008).

Conclusions about the structure's stability were made on the basis that the models showed tensile stresses that exceeded the capacity of the material. It is important to recall that, despite the high tensile stresses predicted by the finite element models, the structure has stood for nearly 2000 years without the inclusion of reinforcement. With this in mind, it is difficult to accept that the hall is weak based on the presence of cracks which have existed at least since the 1930's when they were first documented, and most likely for several hundred years before that, and perhaps even for the 1900 years after the monument was first constructed. Due to the nature of concrete and the geometry of the structure, it is possible that several cracks developed during the original construction or shortly after due to support settlements. Yet, the hall has stood since then without collapse. Therefore, modeling the hall as an elastic continuum and measuring stresses seems to be an oversimplified way of trying to understand the behavior of such a complex and formidably durable building.

Croci determined that the presence of tensile stresses in the model meant that there was strong potential for failure and he proceeded to install metallic hardware throughout the structure without questioning the building's obvious resilience. Despite this, Croci's paper indicates that the implementation of the reinforcement was done with the understanding that localized strengthening procedures would alter the overall structural behavior. He states that the installation was designed to create global stability while being removable should future alterations be required (Croci, et al., 2008). This philosophy demonstrates some sensitivity towards the fact that historic structures should be handled carefully and with considerable

17

foresight. His apparent disregard for the fact that cracks in historic masonry are generally not an indication of impending failure and that material stresses are not a dominant issue for such structures is then perhaps surprising, and the need for steel reinforcement should have been reevaluated. For a monument of such global importance, multiple engineers should be consulted, as in the case of the Tower of Pisa, for example.

3.2   Role of the Lateral Arches

Two of the studies of the hall examine the role of the lateral arch (see Figure 5.2) in the stability of the overall structure. Previous qualitative studies have concluded that the lateral arches act as flying buttresses to transfer the thrust of the vault to the outer wall. One study from the 1920's by Giovannoni made use of graphic statics (see Appendix A – Thrust Line Analysis for more information) and determined that the lateral arches help to keep the thrust lines within the material of the vault (Brune, 2010).
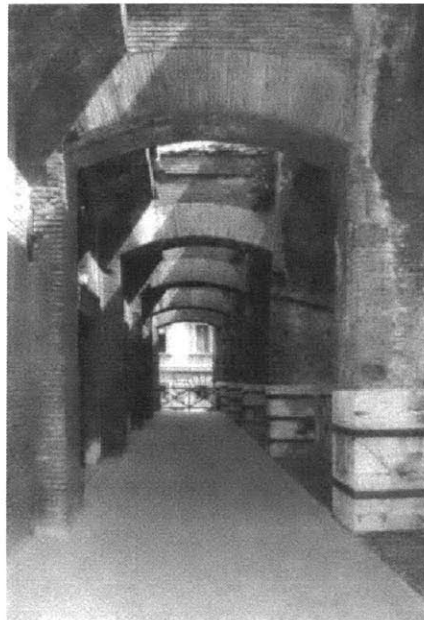
Figure 3.2. View down upper-level corridor with lateral arches overhead (Lancaster, 2005).

In the following, two different methods of evaluation of the vault and its supporting structures are described, as well as the diverging conclusions on the effect of the lateral arches on the behavior of the vault.

18

3.2.1 Method of Funicular Polygons

In a study by Ungaro et al. (2008), a static analysis developed for masonry arches was used as an alternate method to FEM in an attempt to determine the stability of the main vault in its undamaged state. An interior section of the vault (as in Figure 5.9) was taken for analysis under four different configurations:

1. Vault without transverse rib or orthogonal barrel vault (Figure 3.3a)
2. Vault without transverse rib, with lateral arches (Figure 3.3b)
3. Vault with transverse rib, without lateral arches (Figure 3.3c)
4. Vault with transverse rib and lateral arches (Figure 3.3d)
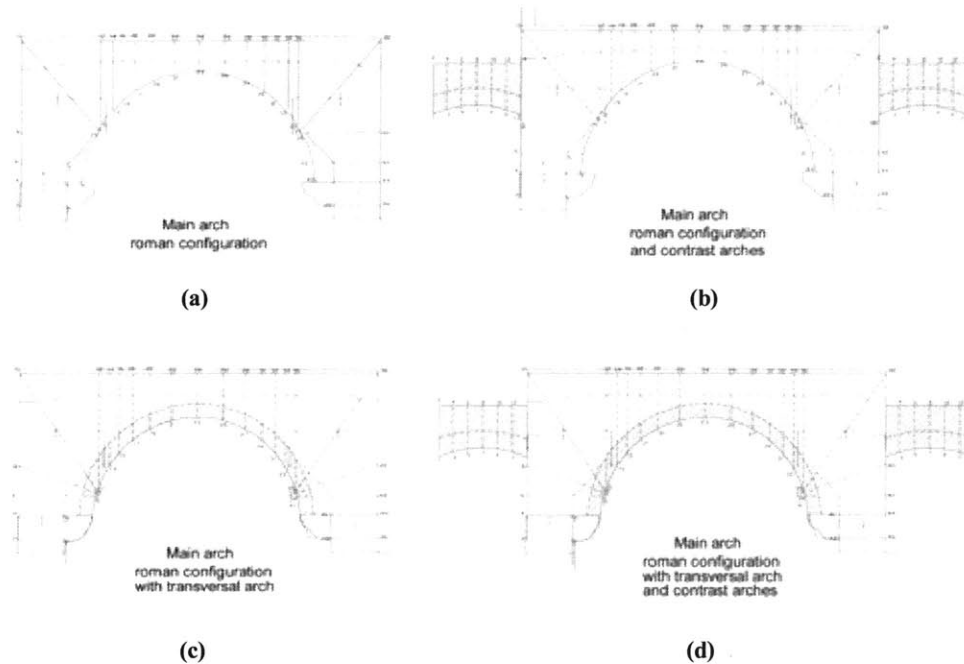
Figure 3.3 Four configurations used for analysis by Ungaro et al. (2008).

A specific weight was applied to the main vault and travertine blocks, as well as extra distributed loads to account for miscellaneous structural features. The cross-vaults were modeled as two orthogonal barrel-vaults and their behavior was analyzed both independently and in combination. The lateral vault section (equivalent to the profile shown in Figure 5.3) was divided into sections and a range of funicular polygons was found (see Appendix A – Thrust Line Analysis). The resultants were then applied to the orthogonal vault to determine its funicular polygons (referred

to in this paper as thrust lines or force resultants, shown in Figure 3.4). Force resultants from supporting elements such as the lateral arches were then added in to create more complex and accurate models. The software used for the analysis calculated many possible funicular polygons for each configuration in conjunction with corresponding sliding coefficients and stresses along the lines of thrust, assuming that tensile stresses could not be sustained by the structure. The solutions were then evaluated and the 'most likely' state was selected for analysis (Ungaro, et al., 2008). For example, the minimum thrust line (dashed line in Figure 3.4a) was considered an unlikely state for the vault as there was predicted to be significant sliding and hinging at the vault extrados associated with this state.

(a)   (b)
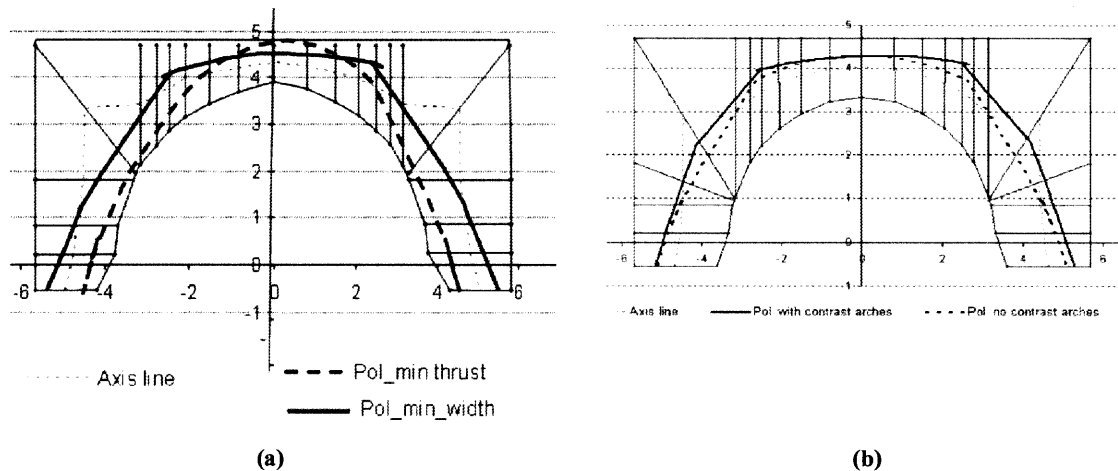
Figure 3.4 (a)Computer results for funicular polygons for scenario 1. (b) Computer-generated results for scenarios 3 and 4 (Ungaro, et al., 2008).

The study makes the main conclusion that the lateral arches slightly improve the stability of the hall by reducing sliding in between the travertine blocks that make up the supporting piers. Figure 3.4b shows an example of the results that led to this argument: the solid line indicates the thrust line with the inclusion of the lateral arches, which is slightly steeper and therefore, an indication of a more stable configuration. The reduction in sliding was found to be especially true for the seismic loading cases. These results are further investigated in this paper using the concept of thrust lines as a guiding principle.

20

The authors also speculate about the presence of 'anti-sliding devices', which could have been metal or wood, placed between the travertine blocks. Their presence is suggested to have two possible reasons. The first is that they may have been put in place following the development of the longitudinal crack at the vault crown after construction caused the vault to thrust on the piers. The second is that they were installed after a major earthquake in 443 B.C.E. which caused sliding between the stones (Ungaro, et al., 2008).

Some of the principles used for analysis in the study by Ungaro et al. are used in the equilibrium analysis presented in this paper, including the concept of thrust lines and the assumption that the material has no tensile strength. Despite the conclusions that the lateral arches improve the stability of the vault and that sliding between the travertine blocks is a significant concern, it is doubtful that there is one true solution for the state of the vault. The selection of one 'most likely' polygon seems somewhat arbitrary, and is not necessarily an indication of the actual state of the present structure.

Although the study states that previous construction work has altered the mechanical behavior of the structure and that earthquake loads are the likely cause of some of the cracks, there is no indication that the authors believe the hall to be currently unstable or unsafe.

3.2.2 Finite Element Method

Similar to the process used by Croci, Brune (2010) analyzed the vault using the Finite Element Method. Brune initially analyzed the vault under gravity loads in isolation from other structural elements and on a rigid base. The study calculated resultant force trajectories through a section of the vault by using software to compute the stresses, strains and displacements and balancing their work done with work done by the internal forces (Brune, 2010). A further study was carried out taking into account the support conditions and the lateral arches in order to observe more realistic behavior of the vaults as a whole (although the effects of the outer buttress are entirely neglected). Conclusions from the first iteration of the analysis showed that a stiff base is required for the stability of the vault. Hence, Brune makes the assertion that the lateral arches should have been located at the vault base near the springing to stiffen the supports at the piers and provide a wider load path (Figure 3.5c). The analysis computed the forces transferred from the vault to the

21

piers and the associated tensile stresses (Brune, 2010). The results showed that the horizontal force of the lateral arch was equal to approximately one quarter of the horizontal reaction at the springing. According to Brune, this indicates that it is the travertine piers that transfer the majority of the vault thrust to the shear wall buttress and that the lateral arches contribute little to the support of the vault.
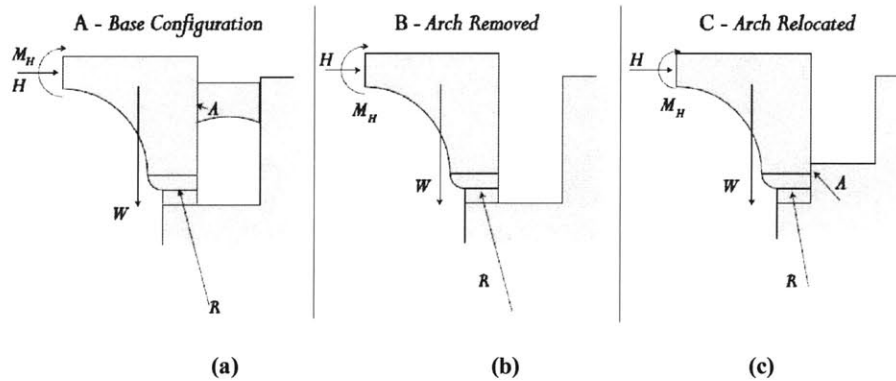
Figure 3.5. (a) Actual configuration of lateral arch. (b) No lateral arch. (c) Position of lateral arch as suggested by Philip Brune (Brune, 2010).

Ultimately, Brune uses Maximum Principal Stresses to judge the effectiveness of the lateral arches. The stress distributions in the lateral arch and vault indicate the presence of significant bending stresses, suggesting that the arches do not help to counter bending in the vault and actually act to the contrary. Brune concludes that the arches have little effect on the analysis results and therefore, have little effect on the stability of the structure in their elevated position. According to his finite element model, moving the arches to the base of the vault, effectively raising the height of the supporting wall, would have a much greater impact on reducing stresses. The thrust values obtained by FEM for the configurations shown in Figure 3.5a and b are as follows:

Actual Configuration (kN)	No Lateral Arch (kN)
159.8	131.9

Table 3.1. Thrust values found by FEM analysis for two lateral arch configurations (Brune, 2010).

22

This study also discusses the importance of sliding between the travertine blocks as a factor in the stability of the hall. If there *is* significant sliding at the pier, moving the lateral arch to the vault base could potentially serve to reduce some of the sliding, although this may be at some other cost to lateral stability. However, this again raises the question of how the hall has stood for so long with the lateral arches in their current positions, if, as stated by Brune, they are in the 'wrong' place.

Brune's results are based on the assumption that the concrete has some tensile capacity, and that there are bending moments throughout the structure. This assumption is unconservative even for the theoretical analysis of modern-day concrete, where the presence of tension leads to cracking. Some of Brune's conclusions agree with those made in the studies by Croci (2008) and Ungaro (2008) such as the fact that sliding plays an important role in the overall stability of the vault and that much of the cracking could have been caused by seismic activity and previous construction work. As with Croci's FEM study, the presence of tensile stress fields is consistent with the locations of actual cracking in the vault.

3.3   Conclusions

The analyses presented above leave several questions unanswered. Each one tries to give one 'true' solution for a structure which is highly indeterminate. It is far more probable that there exists a range of states for which the structure is stable and can stand without danger of collapse. In particular, the finite element analyses rely on material tensile strength to take some of the load exerted by the vault, an assumption which is extremely unlikely given the material properties of concrete and the general behavior of historic masonry structures. The elastic solutions predicted by Finite Element Analysis are highly sensitive to very small and unknowable movements of the supports, making results somewhat arbitrary subject to the user's inputs. These analyses also all make use of fairly complicated computer modeling methods which rely on the user for interpretation. Taking all this into consideration, the analysis presented in this paper makes use of a simpler approach that does not require complex digital modeling. Furthermore, it will provide a range of possible solutions rather than trying to find just one that is assumed to represent the actual state of the vault.

4 Equilibrium Methods versus Linear Stress Analysis

4.1 Stability versus Stress

There are several different methods used for the analysis of structures; which of these methods is employed is dependent on the situation and the assumptions that are relevant to a particular application. Two of the analyses of the Great Hall mentioned above have been made using Finite Element Methods as described in § 3. There is some question as to how meaningful analysis methods such as FEM are for unreinforced masonry structures, where solid objects are modeled as isotropic elastic continua, a highly inaccurate description of materials such as Roman concrete which is an irregular material with complicated properties. Furthermore, the analysis of masonry is generally considered to be an issue of stability and equilibrium; historic masonry structures rarely fail due to lack of material strength and even visible cracks generally do not affect the integrity of the structure (Heyman, 1995). Stresses in masonry are commonly an order of magnitude less than required for the crushing of stone (DeJong, 2009). Therefore, FEM may not be the ideal method of analysis for the Aula Grande. In this paper, equilibrium methods are used to define the limits of stability for the structure and compared to the results obtained from pervious FEM analyses.

To demonstrate the utility of stability rather than stress analysis for historic masonry, an example of two stacked blocks is presented below. Intuitively, one can ascertain that the top block will fall off the base at some critical value of the load P. However, it is not evident whether the block simply falls over the edge or slides before falling nor what the critical value of P is. These are clearly matters of stability and problems that cannot be solved by using linear elastic modeling.
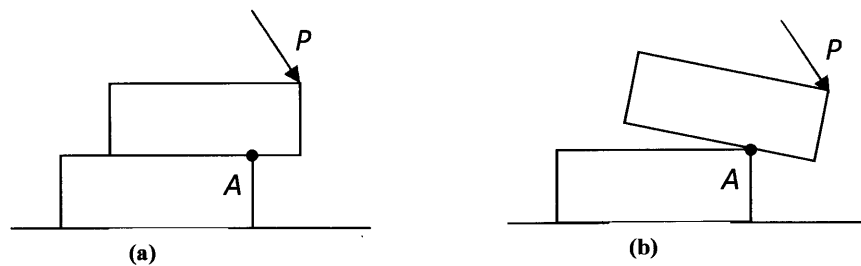

Figure 4.1. Example of stability analysis (John Ochsendorf, personal communication, May 2011).

24

4.2 Theory of Equilibrium Analysis for Historic Masonry

For the analysis of unreinforced masonry where stresses are not a governing issue, equilibrium methods are perhaps more appropriate for the study of historic structures where loads are transferred in compression to arches and vaults rather than slabs and beams as in modern construction (DeJong, 2009). The analysis carried out in this paper relies on using principles of equilibrium to determine the stability of the structure, and then translates the results into a graphical representation in the form of thrust lines.

A masonry structure can be divided into independent blocks ('voussoirs'), which are assumed to act in accordance with three governing assumptions (Heyman, 1995):

1. The blocks have no tensile strength. This assumption is conservative, but made on the basis that the mortar in between the stones is weak and therefore, tensile forces would separate the structural elements.
2. The blocks have infinite compressive strength. This assumption is valid considering that stresses generally remain low in masonry construction, though it can be verified in critical locations.
3. Sliding does not occur between the blocks. Although there is sometimes evidence of sliding between stones, masonry structures generally maintain their shape over time due to sufficient friction between masonry units (Heyman, 1995).

Using these assumptions, graphical and numerical methods were developed to determine the state of specific masonry structures. In order for a masonry structure such as an arch or vault to remain stable, the forces must remain within the material. If at any point the force leaves the confines of the material, a 'hinge' is formed at that location and rotation could occur, leading to a possible collapse mechanism if enough hinges are formed (Block, et al., 2006). In reality, these hinges are seen as cracks either at the intrados or extrados of the arch or vault and may be closed up by the natural expansion of the material into the cracked space (Figure 4.2). Arches with up to three hinges are stable and the cracking associated with the formation of such hinges is not necessarily an indication of imminent collapse (Heyman, 1995).
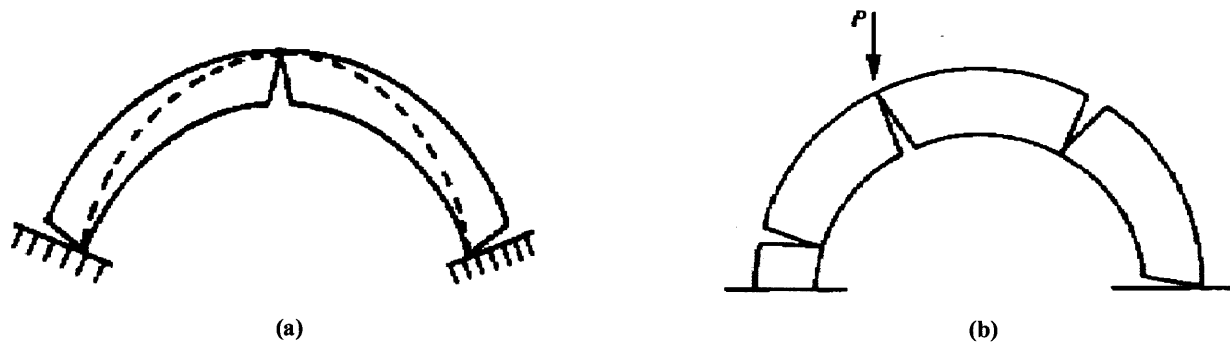
Figure 4.2. (a) Stable state of a cracked arch. (b) Collapse mechanism for a masonry arch (Heyman, 1995).s

The resultants of the compressive internal forces can be visualized as lines of thrust that pass somewhere within the structure's thickness (Block, et al., 2006). The idea of thrust lines comes from a principle first published by Robert Hooke in 1679 which translates to "as hangs the flexible line, so but inverted will stand the rigid arch" (Lancaster, 2005). If weights are hung on a flexible cable, the cable will take a certain shape (funicular shape). If this shape is made rigid and inverted, it represents the line through the equivalent arch through which forces are transferred perfectly in compression i.e. the line of thrust. Hinges are formed when this line touches the extrados or intrados of the arch, and eventual collapse can occur as described above(Heyman, 1995). The graphical method for obtaining the line of thrust was developed in 1866 and is presented in Appendix A – Thrust Line Analysis.

In general, historic buildings are statically indeterminate and there exist an infinite number of paths via which the loads can be transferred to the supports. The analysis of the Aula Grande that follows seeks to find the maximum and minimum of the range of possible values that the structure can support while remaining stable. An arch with up to three hinges is stable and statically determinate. The line of thrust can be found as it must pass through the points of the hinges, since these are the only locations that can transfer forces (Heyman, 1995). For a given line of thrust, the horizontal component of the abutment reaction can be calculated. Figure 4.3 shows the arch under a state of minimum and maximum thrust states; H_{min} is the state most relevant to masonry vaults, and it is the hinge at the crown associated with this state that can be seen on the intrados of the Great Hall vault in the form of cracking. At some critical value of

applied load, the thrust line will leave the bulk of material, forming enough hinges to lead to collapse (Heyman, 1995). The theory for a semicircular arch can be extended to the barrel-vault, which is simply an extrusion of a semicircular arch.
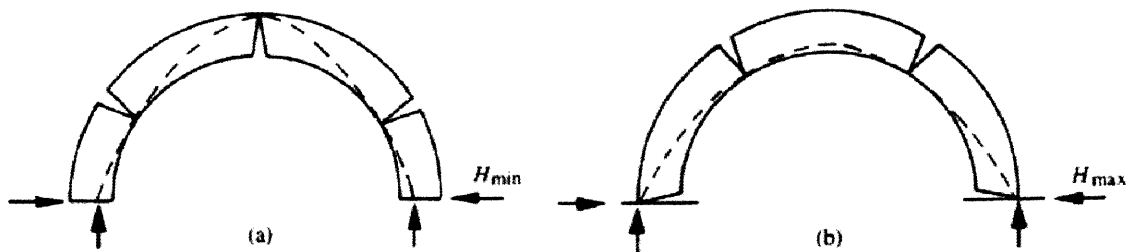

Figure 4.3. A semi-circular arch under its own weight. (a) Minimum abutment thrust. (b) Maximum abutment thrust (Heyman, 1995).

5 Analysis of the Great Hall and General Assumptions

In order to find the limits of stability for the vault, equilibrium methods were used as described below. Three main components that make up the vault and supporting structure (the lateral arch and buttress, which is actually the upper part of a larger shear wall) are analyzed individually and as a system. In this way, the results from the individual pieces could be compared to those of the cohesive structure. There are three possible modes of failure for the vault that are studied below: overturning due to a maximum thrust state, overturning due to a minimum thrust state, and sliding between the travertine blocks at the base of the vault.

5.1 Geometric Assumptions

In order to set up the analysis, a three-dimensional Rhinoceros model, generously provided by Philip Brune, was used to obtain approximate dimensions required for the analysis (Figure 5.2). This model was created under several assumptions that were inherently preserved for the analysis presented in this paper. The geometry was assumed to be that of the supposed original Roman construction, and the damage incurred from its 2000-year life is not included (also assumed by Ungaro (2008)); Figure 5.1 shows the vault in its current state and the version used for analysis.

Dashed outline of section used for computational model

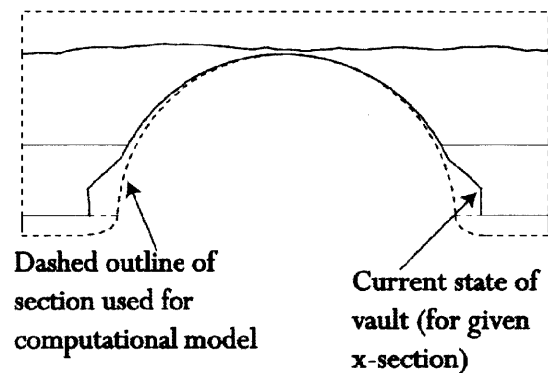Current state of vault (for given x-section)

Figure 5.1 Diagram of geometric assumption made for the analysis model. The dashed line shows the geometry used in the model (Brune, 2010).

As shown in Figure 5.2, the third floor and basement levels are neglected from the model (compare to

28

Figure 2.1c) as these do not dramatically affect the structural behavior of the vault.
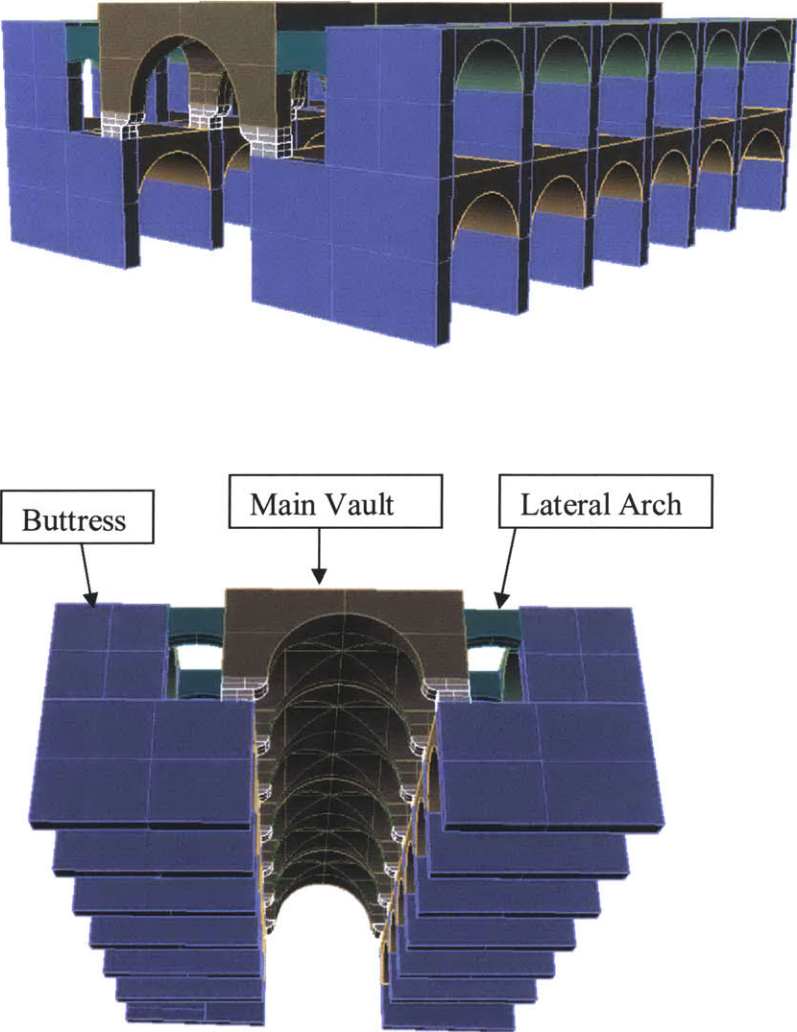
Figure 5.2 Perspective view of the Great Hall of Trajan's Market (Brune, 2010).

Figure 5.3 shows the dimensions applied to the equilibrium analysis, which was limited to the components above the solid line at the base of the vault. The three major elements considered for analysis were: the main vault, the buttress and the lateral arch (indicated with dotted lines in Figure 5.3). Each component was analyzed separately and then in combination to assess the integrated behavior of the system.

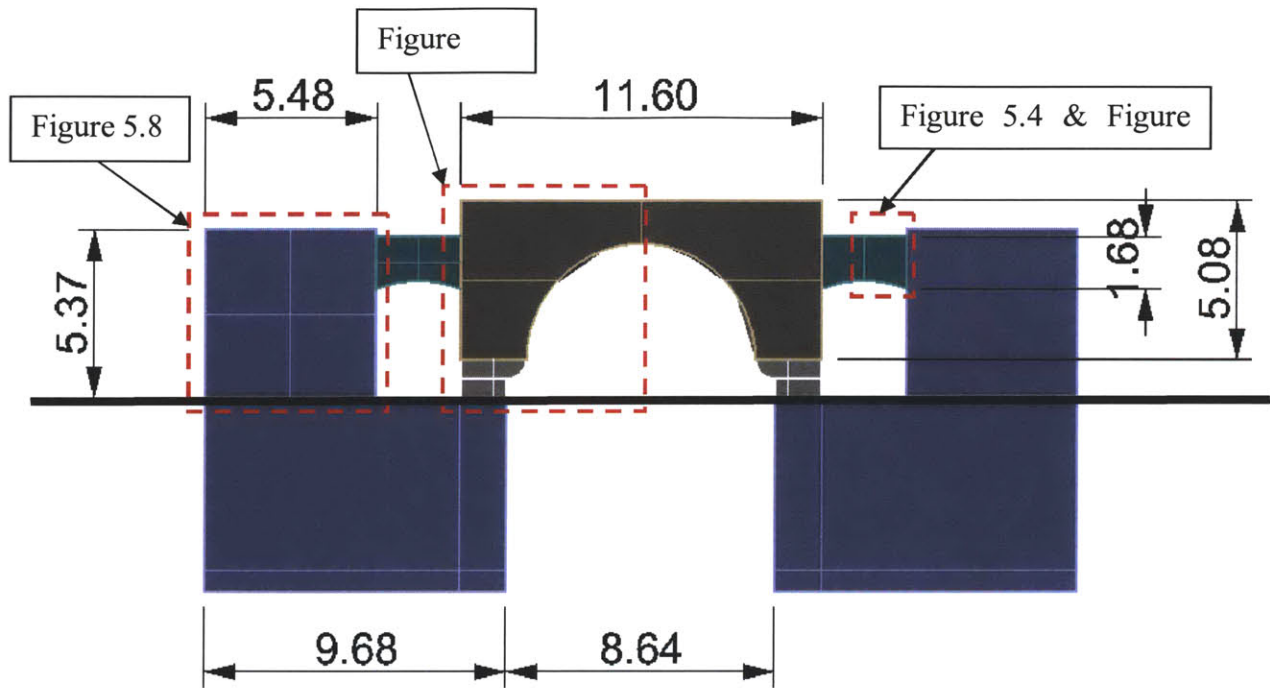**Figure 5.3. Lateral view of the Aula Grande with dimensions in meters. (Brune, 2010).**

5.2 Materials Assumptions

The material properties are adapted from Brune (2010):

Material	Density (kN/m³)	Compressive Strength (MPa)	Tensile Strength (MPa)
Main Vault	13	5	0.5
Travertine	24	50	5
Walls/ Lateral Arches	18	5	0.5

Table 5.1 Material Properties

The strength values are said to be conservative, although the tensile strength of the concrete has never been measured on a structural scale (Brune, 2010). Equilibrium analysis does not rely on the tensile strength of the material, so it is not considered in this paper. In addition, the brick facing on the piers was not treated separately from the material of the main bulk of the vault.

5.3 Formulation of Analysis

5.3.1 The Lateral Arch

$H_{min,arch}$ is the more relevant value for the purpose of this analysis as the thrust line associated with a hinge at the vault extrados relates to the cracking present in the vault. Figure 5.4b shows that a straight line can be drawn through the voussoir, implying that the value of $H_{max,arch}$ is infinite. This is a purely theoretical value, which is limited in reality by the compressive strength of the concrete. Even so, $H_{max,arch}$ is high compared to the values of thrust in the system, and it is unlikely for this to be the cause of failure in the structure.

To determine $H_{min,arch}$, a cut was taken at the midpoint of the lateral arch (indicated in Figure 5.3) and equilibrating forces were applied as shown in Figure 5.4a. The figure shows the diagram used for the set-up of the global equilibrium equations for half of the arch to obtain the value of $H_{min,arch}$ (Equation 5.1). For the minimum thrust state, it was assumed that the hinges would occur at the extrados (point A) and at point E.
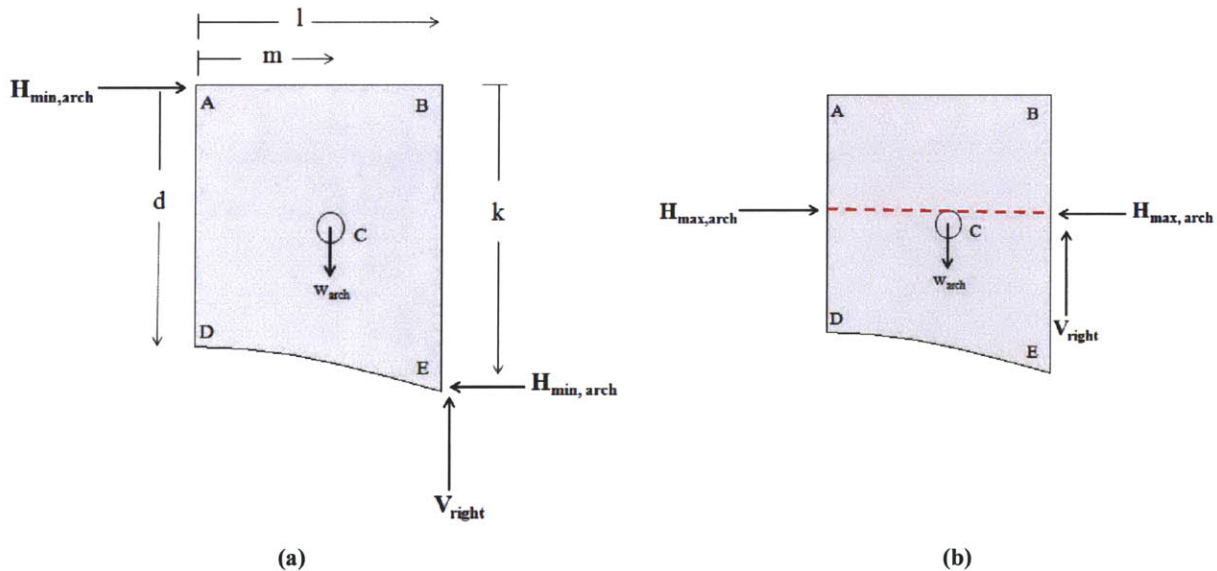
Figure 5.4. Diagram of half of lateral arch used for global equilibrium calculation.

Knowing the value of $H_{min,arch}$, the half-arch was then subdivided into five 'voussoirs', each with its own centroid (point C_i) and weight (w_i). Beginning with the voussoir furthest to the right (voussoir 5), the thrust line begins at point E_i and passes through the boundary somewhere between points A_i and D_i. Using equations of equilibrium (Equation 5.2 and Equation 5.3), the point where the thrust line crosses the boundary into voussoir 4 could be found, and so on

31

through all the blocks until global point A was reached (for full calculations and voussoir weights, see Appendix B – Sample Calculations and Results for Lateral Arch).
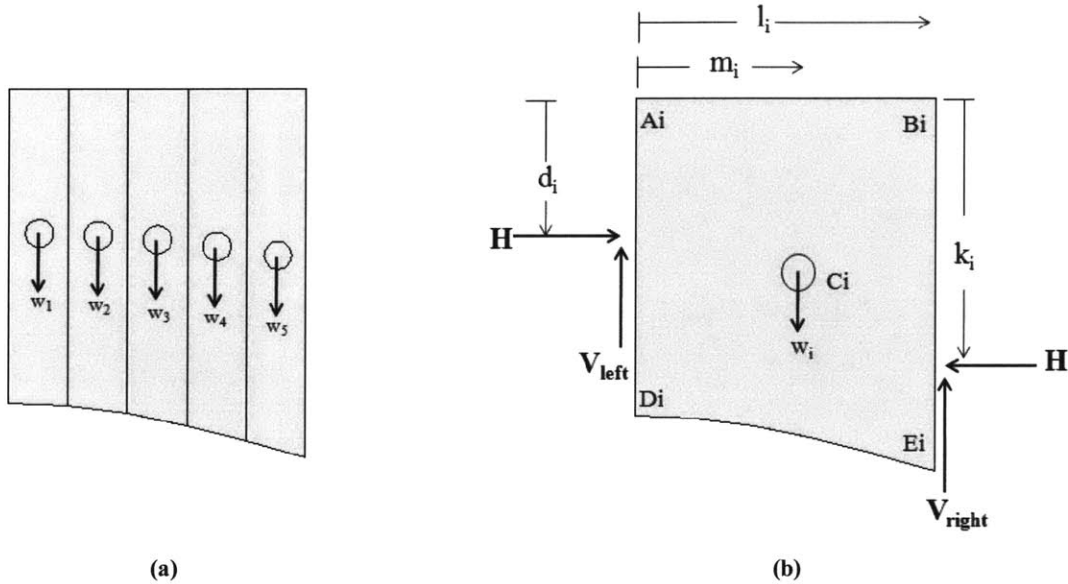
Figure 5.5 (a) Diagram of half-arch divided into five voussoirs showing the individual weight through each center of mass. (b) Equilibrium forces of a generalized voussoir.

Global Equilibrium

Taking moments about point A, $\sum M_A = 0$

$$H_{min,arch} = \frac{w_{T/2}l - w_{T/2}m}{k}$$

Voussoir Equilibrium (Refer to Figure 5.5)

Summing forces in the vertical direction, $\sum F_y = 0$

$$V_{left_i} = w_i - V_{right_i}$$

Taking moments about point A, $\sum M_A = 0$

$$d_i = \frac{w_i m_i + H_{min}k_i - V_{right}l_i}{H_{min,arch}}$$

Where

- $w_{T/2}$ = total weight of half of the arch
- V_{left}, V_{right} = vertical reaction to the left and right, respectively
- w_i = weight of the voussoir
- m = length from pivot to centroid
- l = length of voussoir
- d = distance from pivot to H on the left edge of voussoir
- k = distance from pivot to H on right edge of voussoir
- i = voissoir number (i = 1, 2, 3, 4, 5, see Figure 5.5a)

(a)

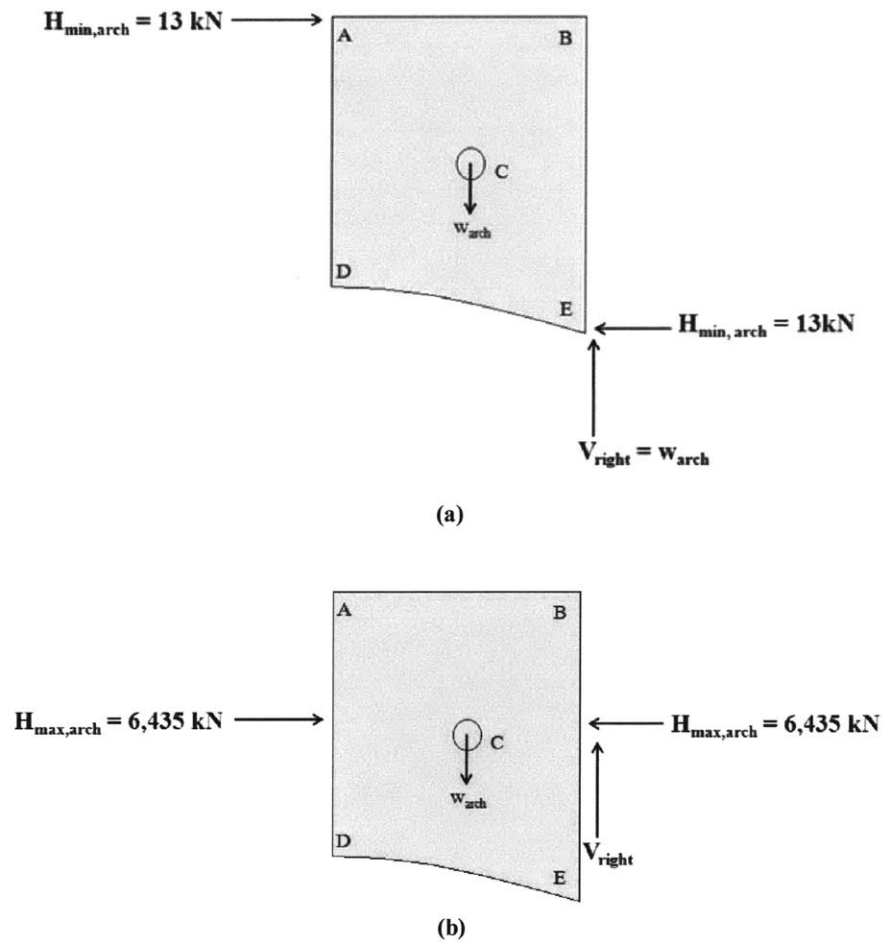

(b)

Figure 5.6 (a) $H_{min,arch}$. (b) $H_{max,arch}$ limited by compressive strength.

33

The table below summarizes the thrust exerted by the lateral arch in its minimum and maximum states, which are illustrated in Figure 5.6.

$H_{min,arch}$	13	kN	
$H_{max,arch}$	∞	kN	Theoretical value. This is actually limited by the compressive strength of the concrete.
$H_{max,arch}$	6,435	kN	Value limited by compressive strength of material[1].

Table 5.2 Hmin and Hmax for lateral arch.

Figure 5.7 shows the path of the resultant force passing through the lateral arch in its minimum thrust state.

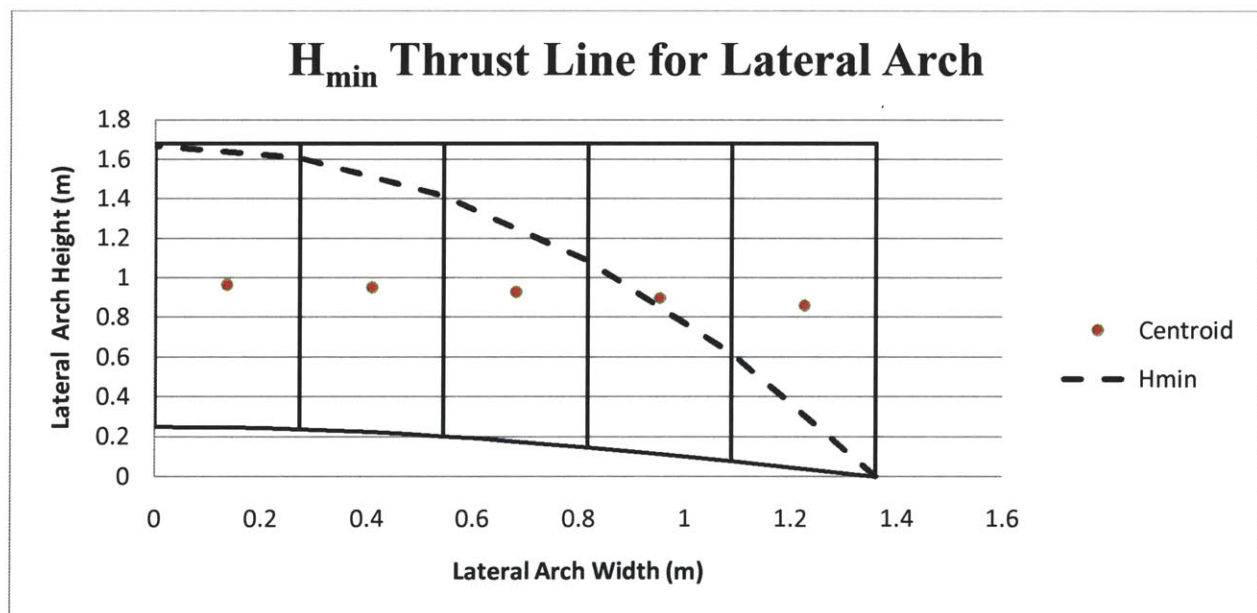**Figure 5.7 Minimum thrust line for the lateral arch.**

---

[1] This value is calculated as follows: $F = \sigma A = 5000$ kPa $\times 1.29$ m^2 = 6,435 kN
  where σ = strength of material, provided by Brune (2010)
    A = smallest area of the arch.

5.3.2 The Buttress

Another supporting element of the vault is the 'buttress', which is the upper part of a larger shear wall (shown in Figure 5.3). The buttress was analyzed under the assumption that the lateral arch is modeled as a rigid link that only transfers force horizontally between the buttress and vault. The limiting state for the buttress is its overturning about point D corresponding to a state of maximum thrust. H_{max} is calculated as follows:

Taking moments about point D_b, $\sum M_{Db} = 0$

<div align="right">Equation 5.4</div>

$$H_{max,buttress} = \frac{w_b m}{k}$$
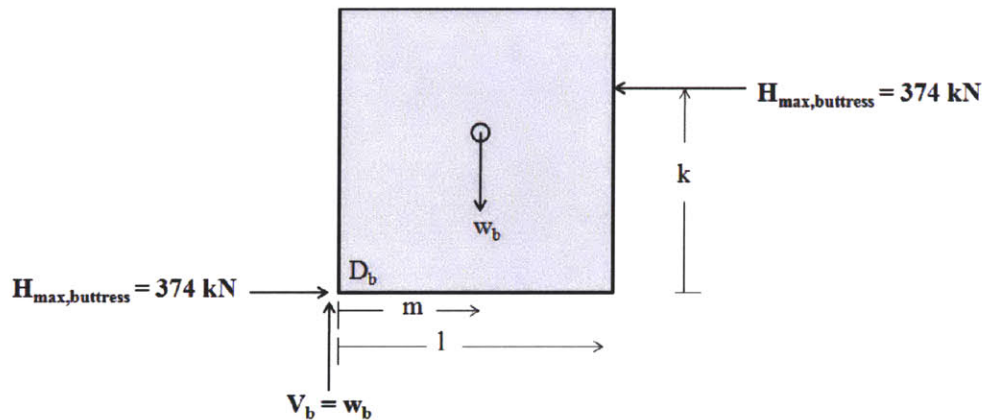
Figure 5.8 Equilibrium analysis of the buttress.

The value for k was taken to be 3.49m, the distance where the bottom of the arch meets the buttress. The results are shown in Table 5.3 below.

| | w_b | m | k | $H_{max,buttress}$ |
	(kN)	(m)	(m)	(kN)
Overturning	477	2.74	3.49	374^2

Table 5.3 Hmax for the buttress.

---

[2] This can be reduced by 30% due to part of the buttress being ineffective in this limit of overturning (Ochsendorf, et al., 2004).

5.3.3   The Vault

A similar analysis as was carried out for the arch and buttress was applied to the vault to determine H_{min} and H_{max} with various support conditions (i.e. with the arch and the buttress or without).

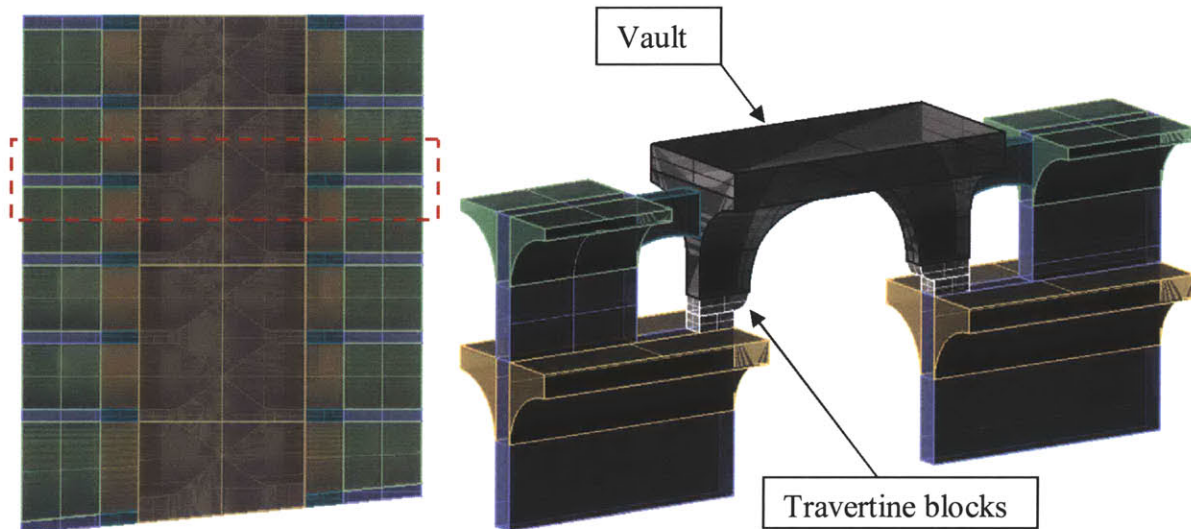**Figure 5.9. Section of vault used for analysis.**

Due to the complex geometry of the cross-vaults, they had to be simplified to two-dimensional slices for analysis: the complex barrel vaulting was neglected and replaced with a simple thickness equal to the depth of the piers, while the lateral profile was maintained. With the Rhinoceros drawing software, the volume of a section of vault equal to the tributary area of one set of piers was found (Figure 5.9). Using the material properties of Roman concrete and travertine shown in Table 5.1, the weight of the vault (including the travertine blocks) was calculated. For the initial analysis, it was assumed that the travertine piers behave monolithically with the rest of the vault. The weight of the actual section was calculated and used to obtain an equivalent density for the simplified 2D model. This equivalent density was applied to the vault to simulate the mass of the vault thrusting on the supports. As the vault is practically symmetrical, it was assumed that the centroid of the model would be in a similar location with respect to the supports as the centroid of a geometrically accurate section.

The thrusts of the vault were calculated in a similar manner to that described in § 5.3.1: the vault was divided into five sections (Figure 5.10a) which were analyzed one by one. The thrust lines were then plotted to ensure that they remained within the thickness of the material.

5.3.3.1 Equations for Vault Equilibrium (Vault Only)
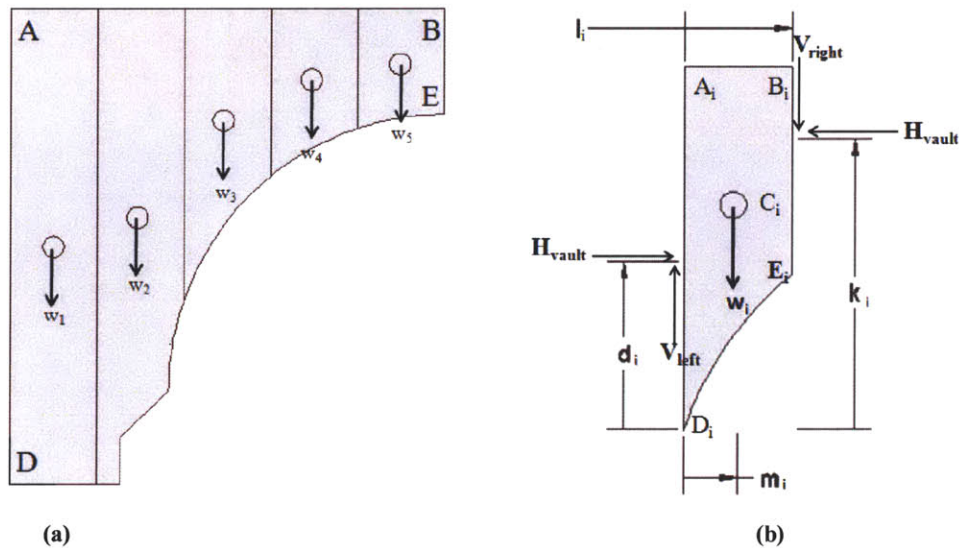
Figure 5.10 (a) Half-vault divided into five voussoirs. (b) Individual voussoir with generalized dimensions and forces.

- $w_{T/2}$ = total weight of half of the vault
- V_{left}, V_{right} = vertical reaction to the left and right, respectively
- w_i = weight of the voussoir
- m = length from pivot to centroid
- l = length of voussoir
- d = distance from pivot to H on the left edge of voussoir
- k = distance from pivot to H on right edge of voussoir
- i = voissoir number (i = 1, 2, 3, 4, 5, see Figure 5.10a)
- H = H_{min} (Figure 5.11a) or H_{max} (Figure 5.11b)

Global Equilibrium

Taking moments about point D, $\sum M_D = 0$

37

Equation 5.5

$$H_{vault} = \frac{w_{T/2}m}{k}$$

Voussoir Equilibrium

Summing forces in the vertical direction, $\sum F_y = 0$

Equation 5.6

$$V_{left_i} = w_i - V_{right_i}$$

Taking moments about point D, $\sum M_D = 0$

Equation 5.7

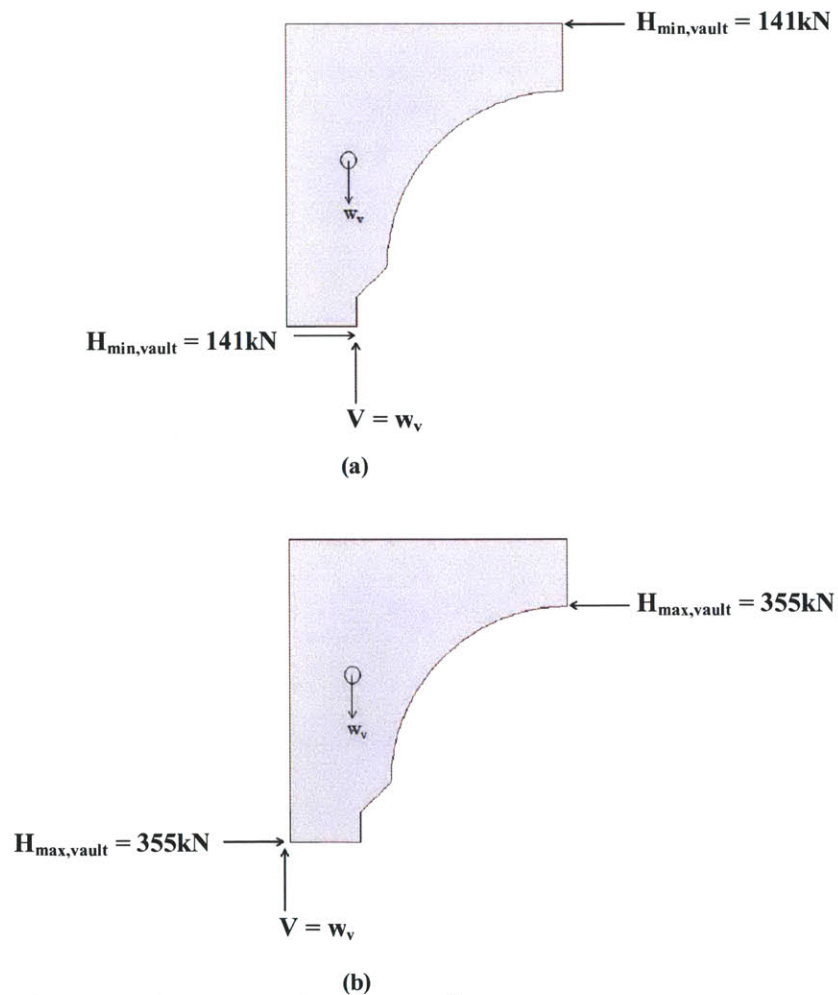$$k_i = \frac{w_i m_i + H d_i + V_{right} l_i}{H_{vault}}$$

(a)

(b)

Figure 5.11 (a) H_min, vault and (b) H_max,vault for the vault without supporting structures.

38

| | $H_{min,vault}$ | $H_{max,vault}$ |
	(kN)	(kN)
Vault Only	141	355

Table 5.4 Values for vault without connection to buttress.

5.3.3.2 *The Vault with Supporting Structures*

For the final stage of the analysis, the buttress and the lateral arch were included to complete the system. The buttress imposes a limit on the stability of the system and is a crucial element in understanding the overall structural behavior. The limiting state of the system was taken to be rotation about points D_b (Figure 5.12) for the case of some maximum horizontal force being applied to the vault. In calculating H_{max} (§ 5.3.3.2.2), it was assumed that the arch acts as a rigid link which is pinned between the buttress and the vault and can only transfer force horizontally (Figure 5.12). This assumption means that the vault and buttress rotate as rigid bodies about their respective pivot points. There is a second assumed limiting state for a minimum horizontal thrust value, wherein the vault rotates about point E_v. The respective limiting horizontal values are then solved for as described below to determine the limits of stability.
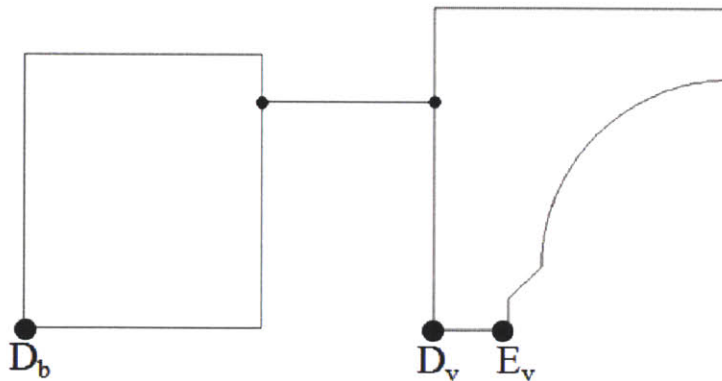
Figure 5.12. Complete system with horizontal link in place of the lateral arch.

5.3.3.2.1 System H_{min}

The system H_{min} corresponds to the scenario where the lateral arch is included. In this case, the thrust line touches the extrados of the lateral arch (assumed in the middle of the arch length, which is the location of a hinge. The resultant force exerted by the lateral arch is applied to the

vault at an angle θ, the angle formed by the resultant at the edge of the lateral arch (Figure 5.13b). This force is resolved into a horizontal and vertical force for equilibrium analysis.
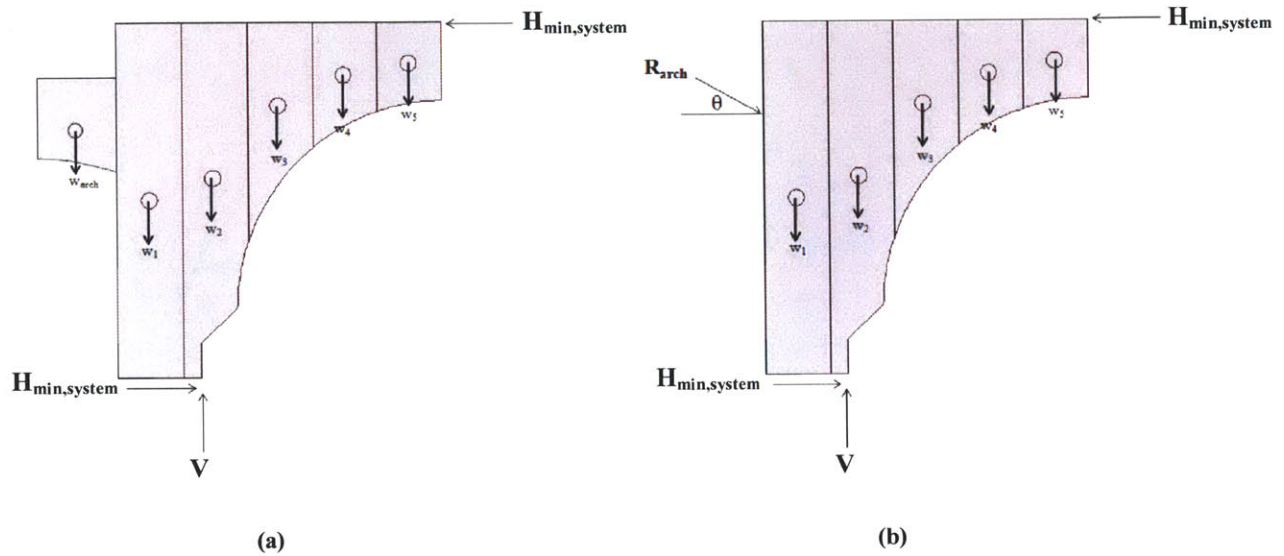
Figure 5.13 (a) Vault in minimum thrust state with lateral arch. (b) Equivalent diagram used for analysis with resultant force from the arch thrust.

The equilibrium equations for this case are similar to those where the lateral arch is not present, except that the horizontal and vertical effects of the resultant from the arch must be included. The thrust lines for the vault with and without the supporting arch are plotted in Figure 5.14.
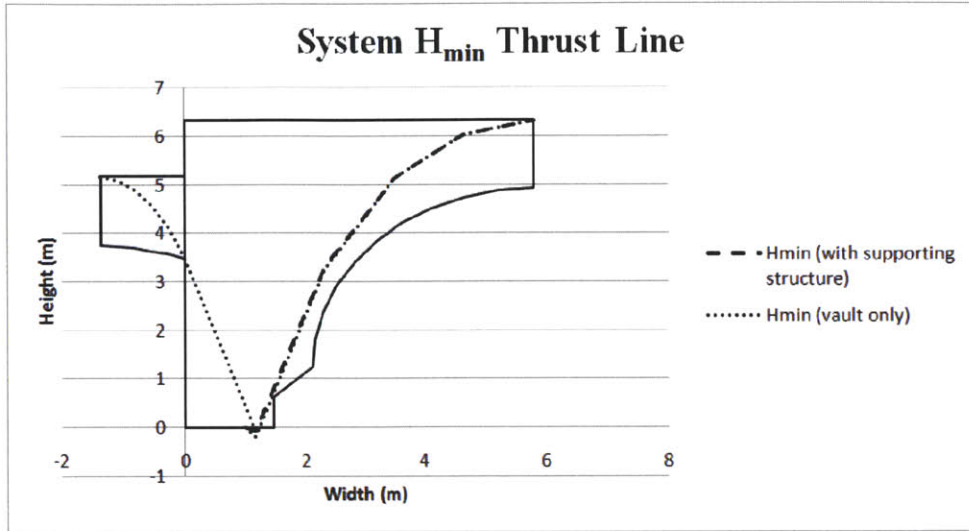
Figure 5.14 H_{min} for the vault only and the vault with the supporting system.

5.3.3.2.2 System $H_{max,system}$

The limiting state of the system for the case of maximum thrust is overturning of the vault about point D_v (Figure 5.15, right) which, in turn, is limited by the capacity of the buttress before overturning about D_b (Figure 5.15, left). Due to the simplification of the lateral arch as a rigid link, the value of $H_{buttress}$ obtained from the calculation for the buttress (shown in § 5.3.2) is transferred directly to the vault and all the forces for the system can be calculated using equilibrium equations and solving simultaneously.
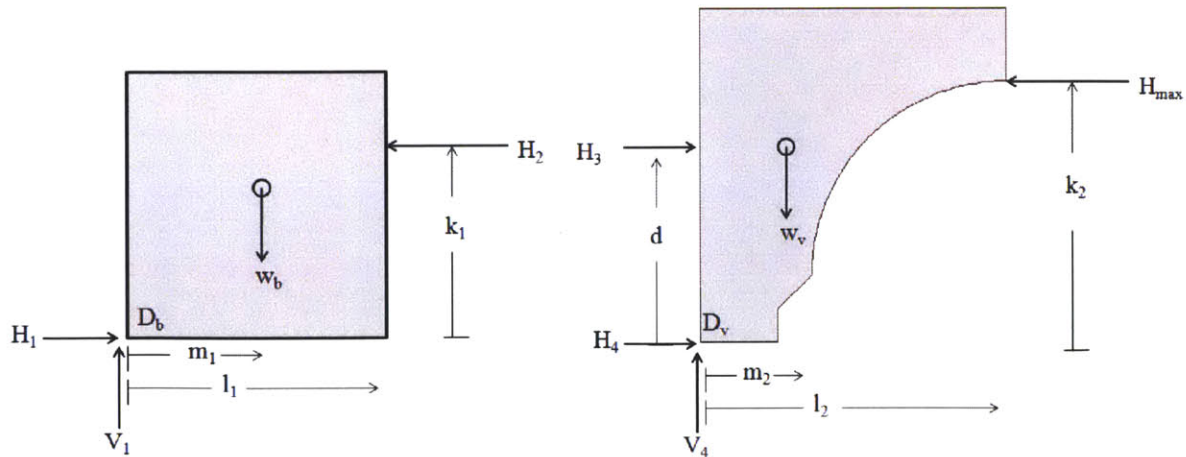
Figure 5.15 Equilibrating forces for the system for the $H_{max,system}$ calculation.

41

The equations of equilibrium are as follows:

Summing forces in the vertical direction, $\sum F_y = 0$

$$H_1 = H_2$$

$$H_2 = H_3$$

$$H_3 + H_4 = H_{max}$$

Summing forces in the horizontal direction, $\sum F_x = 0$

$$V_1 = w_b$$

$$V_4 = w_v$$

Taking moments about respective point D, $\sum M_D = 0$

$$H_2 = \frac{w_b m_1}{k_1}$$

$$H_{max,system} = \frac{w_v m_2 + H_3 d}{k_2}$$

$H_{min,system} = 144kN$

$R_{arch} = 32kN$

w_v

$H_{min,system} = 144kN$

$V = w_v + w_a$

(a)

$H_{max,system} = 621kN$

$H_{max,buttress} = 374kN$

w_v

$H_{max,system} = 621kN$

$V = w_v + w_a$

(b)
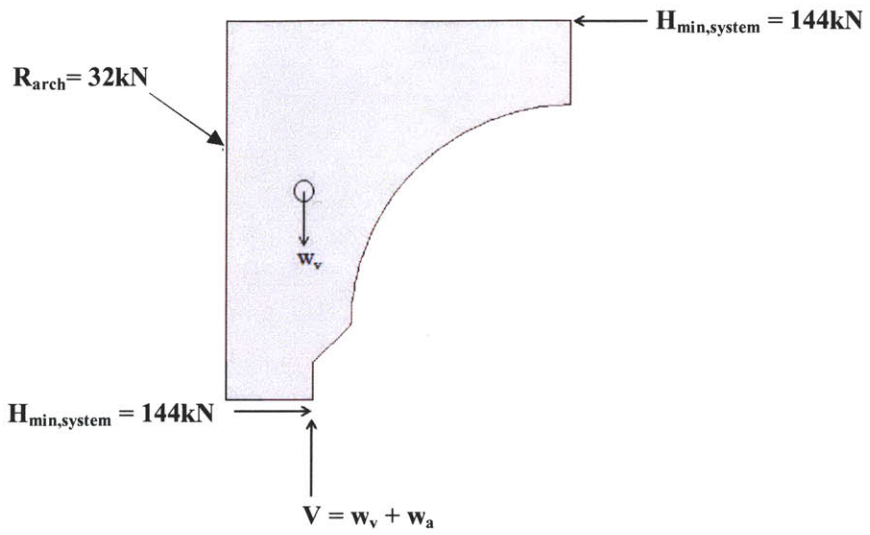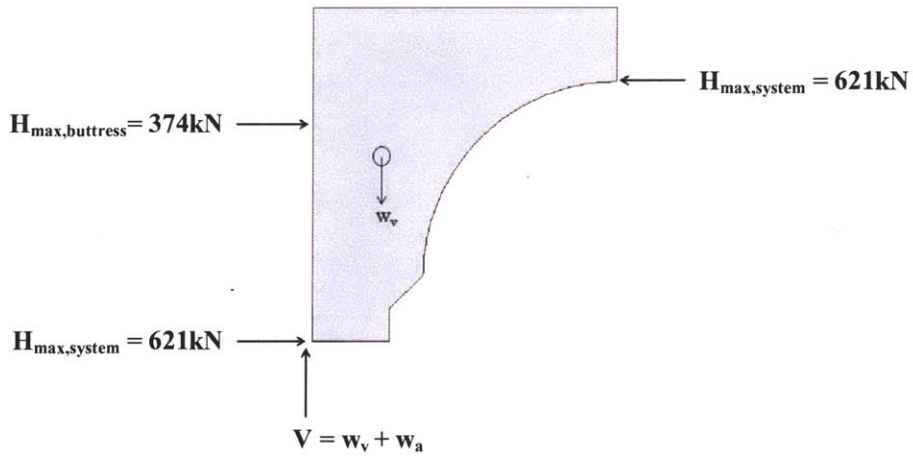
Figure 5.16 (a) $H_{min,\,vault}$ and (b) $H_{max,vault}$ for the vault with the supporting structures included.

	$H_{min,system}$ (kN)	$H_{max,system}$ (kN)
Vault + Support	144	621

Table 5.5 $H_{min,system}$ and $H_{max,system}$ for vault with supporting structure included.

Figure 5.17 shows the thrust lines for the vault in its state of maximum thrust with and without the buttress. The thrust line associated with the vault (supporting structure included) is steeper, indicating a more stable system.
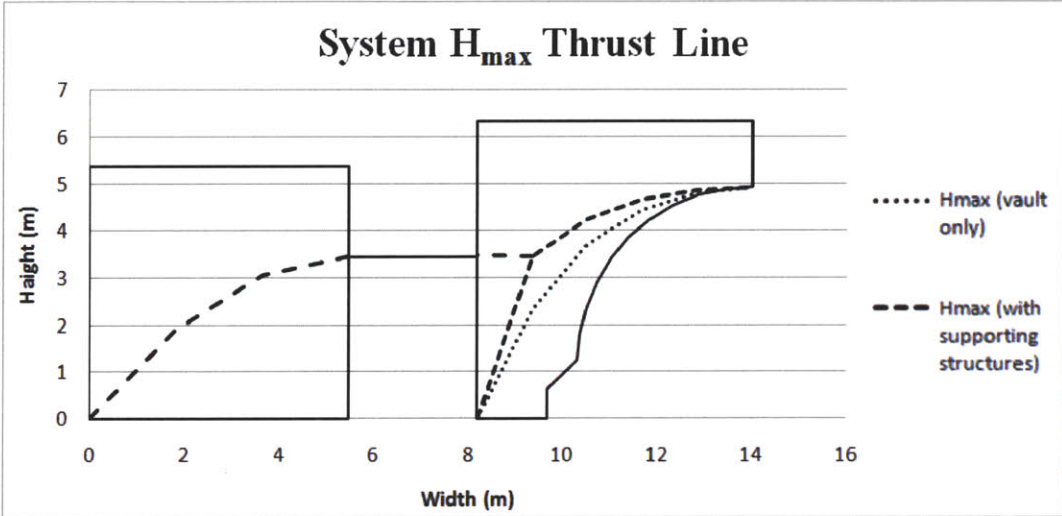
Figure 5.17 H_{max} for the vault only and the vault with the supporting system.

5.4 Sliding

One of the concerns raised in the literature was that of sliding between the travertine blocks which could cause instability in the support structure. A simple analysis was carried out to determine whether sliding is likely between blocks comprising the pier and is described diagrammatically in Figure 5.18.
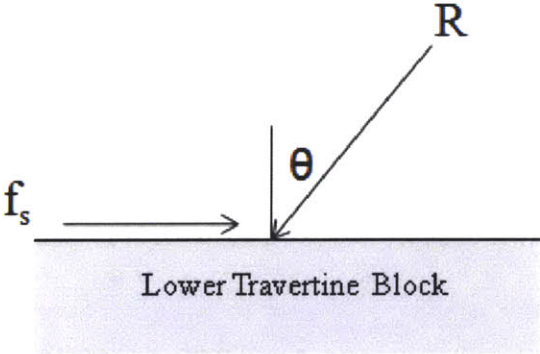
Figure 5.18. Forces of friction on a block representing the lower block of the pier.

The weight of the vault plus the weight of the upper travertine block (w) bear down on the lower travertine block. Their combined weight leads to a vertical reaction (N) which, referring to Figure 5.18, is equal to Rcosθ. A static friction force (f_s) opposes the applied horizontal force (H = Rsinθ) up to a limit where f_s is equal to H. Thus, the equations are written as follows:

Equation 5.15

$$f_s = \mu_s N$$

Where

Equation 5.16

$$N = R \cos \theta = w$$

For the limiting state, the angle that will cause sliding is

Equation 5.17

$$\mu_s = \tan \theta$$

Where μ_s = coefficient of static friction and equal to 0.7 (Ochsendorf, et al., 2004). Rearranging and solving for the maximum horizontal force that causes sliding:

Equation 5.18

$$H_{sliding,vault} = R \sin \theta = \mu_s w \cong 592\ kN$$

Using the same method, the maximum amount of force that can be applied to the buttress before sliding occurs was found to be approximately 334kN. Therefore, the amount of force required to cause sliding in the system (vault with supporting structures) is the sum of $H_{sliding,vault}$ and $H_{sliding,buttress}$, which is approximately equal to 926kN.

6 Results and Discussion

	H_{min} (kN)	H_{max} (kN)
1. Vault Only	141	355
2. Vault + Supporting Structures	144	621
3. Sliding (Vault Only)	592	
4. Sliding (Vault + Supporting Structures)	926	

Table 6.1 Comparison of results for the different cases analyzed.

The results shown in Table 6.1 compare the values for the four different cases analyzed: the vault only, the vault with the supporting structures included, and the force required for sliding to occur in the respective scenarios. The values demonstrate clearly that there is a marked increase in the range of values of horizontal thrust that the vault can support under static loading when the supporting structures are present. This shows that the lateral arch and the buttress are crucial members in the stability of the vault. This is emphasized by comparing the values of horizontal force required to cause sliding: when the supporting structure is present, the amount of force is considerably higher. However, the forces required to cause sliding are significantly higher than those where sliding is not a factor, thus, it can be inferred that sliding is not a consideration for the vault under its own weight. Furthermore, the fact that the horizontal force needed to cause sliding is slightly lower than $H_{max,system}$ means that collapse would theoretically occur by sliding between the travertine blocks before the vault could develop its maximum thrust state.

It should be noted that there were several simplifications made in the analysis that would somewhat alter the results. For example, the three-dimensional nature of the complex vault intrados was not taken into account and the travertine blocks were assumed to be monolithic with the vault structure. These assumptions would affect the weights of the voussoirs used to carry out the thrust line analysis. Therefore, the behavior of the actual vault may be rather different to what was assumed in this analysis. In addition, the use of the rigid link in place of the lateral arch in the $H_{max,system}$ analysis neglects the fact that the arch would apply vertical forces to the vault and buttress. The results from this assumption give more conservative values of the capacity of the

46

system, as the vertical component of the arch's reactions would increase the amount of horizontal force that the system can support before collapse. The locations in which hinges would form to create the collapse mechanisms for the maximum and minimum thrust states were also assumed. It is possible, of course, that the vault could fail in an entirely different manner. In addition, the fact that the vault was analyzed in the lateral profile does not take into account the structure's behavior in the longitudinal direction. Despite the various assumptions made, the analysis was carried out without relying on the masonry supporting loads in tension as is assumed, unconservatively, in FEM.

The equilibrium analysis presented above was to successfully provide a range of possible states in which the vault remains stable. Given that the structural system *does* include the lateral arch and the buttress, there is a large range of solutions for which the vault would remain stable, and its collapse under static conditions is unlikely. Although seismic loading was beyond the scope of this project, the conclusions made above lead to the view that the lateral arches and buttresses throughout the hall would have a major impact on the stability of the vault if a seismic event occurred in the lateral direction of the vault. An equilibrium analysis taking into account seismic loading may have been able to provide a broader view than the FEM analyses of the behavior of the structure, and the insertion of metallic reinforcement could potentially have been avoided.

7 Conclusions

There are three main conclusions that can be made from the equilibrium analysis presented in this paper:

1. The range of possible thrust values for the vault increases (from 141-355kN to 144-621kN) when the lateral arch and buttress are included. Hence, they are crucial for the stability of the vault under static loading.

2. Sliding is unlikely to occur under static conditions. (Sliding may occur due to seismic accelerations, in which case the buttress and lateral arch would probably augment the stability of the vault, but this is beyond the scope of this study).

3. Equilibrium analysis is a useful and relatively simple method for the analysis of historic masonry structures that can provide a more informative understanding of their behavior.

8 References

Bianchini, M. "I 'Mercati di Traiano*Bolletino di Archeologia de Ministero per i Beni Culturali e Ambientali*".
(2008), 102-121, http://www.rilievoarcheologico.it/home-articoli-li_g000019.pdf.

Bianchini, M. *"La volta della Grande Aula"*, in L. Ungaro, M.P. Del Moro, M. Vitti (a cura di), *I Mercati di Traiano restituiti. Studi e restauri 2005-2007*, Roma 2010, pp. 45-58, http://www.rilievoarcheologico.it/home-articoli-li_g000021.pdf

Block, P., Ciblac, T., and Ochsendorf J., *"Real-Time Analysis of Vaulted Masonry Buildings."* Computers and Structures 84. (2006): 1841-1852.

Brune, P., *"The Mechanics of Imperial Roman Concrete and Strcutural Design of Vaulted Monuments."* Rochester: 2010.

Croci, G., Viskovic A., Bozzetti, A., Ungaro, L., and Vitti. M., *"The Trajan Markets and their Great Hall - TheConservation Problems and the Strutural Intervention for the Improvement of the Seismic Safety."* Structural Analysis of Historic Construction. (2008)

DeJong , M. J., *Sesimic Assessment Strategies for Masonry Structures.* Cambridge: 2009.

Heyman, J., *The Stone Skeleton: Structural Engineering of Masonry Structures.* Cambridge: Cambridge University Press, 1995.

Lancaster, L. C., *Concrete Vaulted Construction in Imperial Rome.* New York: Cambridge University Press, 2005.

Ochsendorf, J., Huerta S. and Hernando, J. I., *"Collapse of Masonry Buttresses"* Journal of Architectural Engineering, American Society of Civil Engineers, Vol. 10, No. 3, pp. 88-97, September 2004.

Perucchio, R., and Brune, P., "Concrete Vaulting in Imperial Rome: A Structural Analysis of the Great Hall of Trajan's Markets." *Proceedings of the Proceedings of the 6th International Conference on Computation of Shell and Spatial Structures,* Ithaca New York: (2008).

Ungaro,L., Vitti, M., Speranza, E., *"The Great Hall of the Trajan Markets Throughout the Centuries. "* D'Ayala & Fodde. London: Taylor and Francis Group (2008).

Appendix A – Thrust Line Analysis
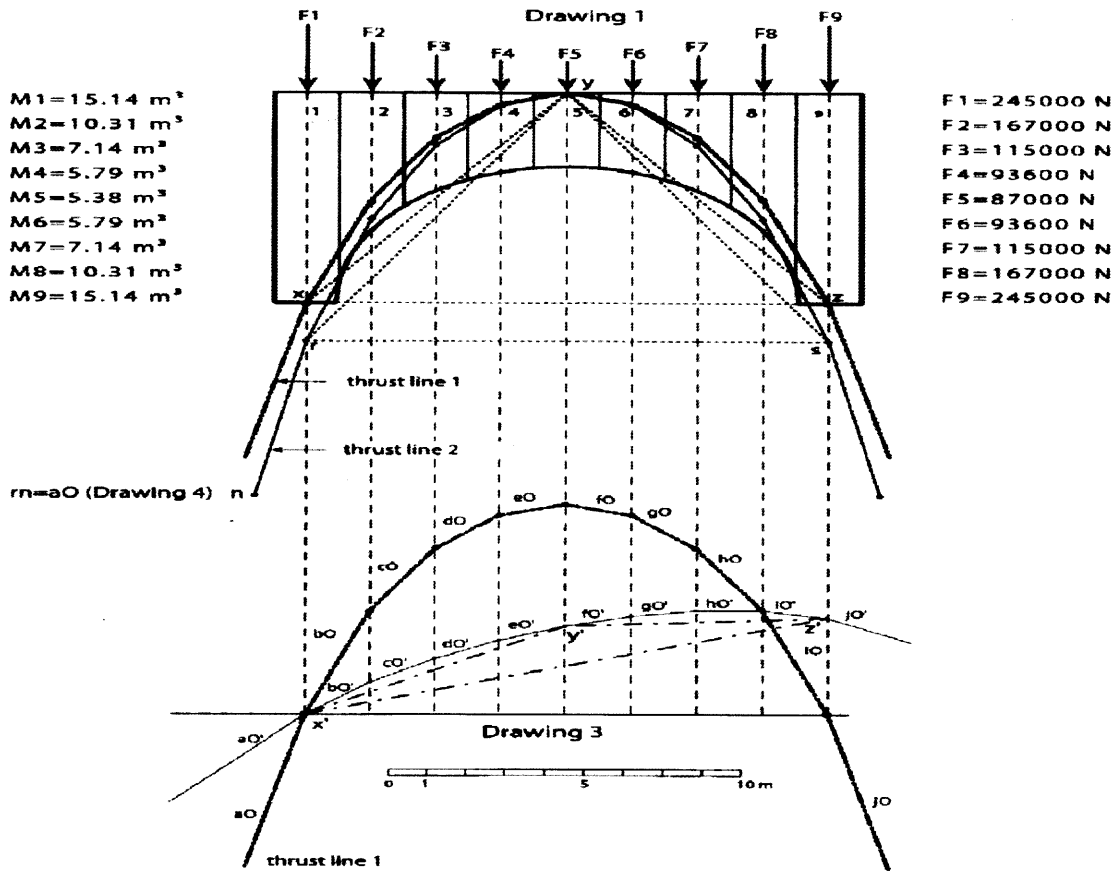
Reproduced with the permission of Lynne Lancaster.

THRUST LINE ANALYSIS

THE FUNICULAR POLYGON METHOD OF THRUST LINE analysis became a standard way of analyzing arches in the nineteenth century when the introduction of graphical methods made it more user-friendly than the mathematical methods with which the principles were developed. I use it in Chapter 8 to test the efficacy of various techniques discussed in this study. In what follows, I provide an example of how to perform a simple thrust line analysis for a barrel vault. It can be done with a pencil and paper, but I use AutoCad for greater accuracy and ease.

PART I

STEPS FOR CONSTRUCTING THE THRUST LINE
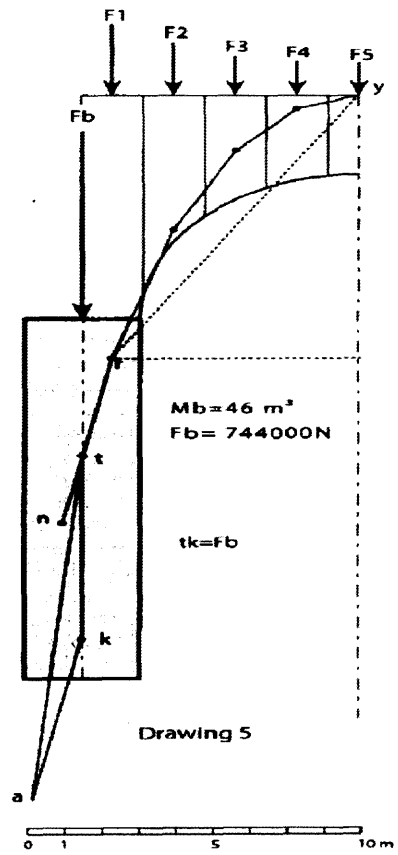THROUGH A BARREL VAULT (FIG. 145):

1. Draw a scaled profile of the vault to be analyzed (shaded area in Drawing 1).
2. Divide the vault into an odd number of vertical sections (the more sections the more accurate the final curve) so that the middle section is centered on the crown of the vault. Number each section starting with "1" at the far left.
3a. Determine the unit weight of the material used for each section in kg/m³. Calculate the mass (M) of each section in m³ and multiply it times the

unit weight of the material used. The weight (W) in kg must then be translated into units of force in Newtons (N) by multiplying by 9.8 m/sec/sec. These are the force vectors, each of which is referred to by the number of its corresponding section, for example, F_1, F_2, F_3, and so on.
3b. To draw the force vectors, choose a convenient scale for the vectors so that each unit in the drawing equals a certain number of Newtons (e.g., scale above Drawing 2). Draw each calculated force vector as point load located at the center of gravity of its section. (A program such as AutoCad can calculate the center of gravity of unsymmetrical shapes automatically.)
4. Out to the side of the drawing of the vault (Drawing 1), draw the force vectors end to end (Drawing 2), one above the other at the same scale as represented on Drawing 1. Then pick an arbitrary point (the trial pole-O′) and connect the ends of the vectors labeled a, b, c, and so on, to O′ so that you have a series of radiating lines: aO′, bO′, and so on (the thin solid lines on Drawing 2).
5. Below Drawing 1, project the line of action of each force down to a base line (Drawing 3). Then starting at the left where the line of action of

Drawing 1

| F1 | F2 | F3 | F4 | F5 | F6 | F7 | F8 | F9 |

M1=15.14 m³
M2=10.31 m³
M3=7.14 m³
M4=5.79 m³
M5=5.38 m³
M6=5.79 m³
M7=7.14 m³
M8=10.31 m³
M9=15.14 m³

F1=245000 N
F2=167000 N
F3=115000 N
F4=93600 N
F5=87000 N
F6=93600 N
F7=115000 N
F8=167000 N
F9=245000 N

thrust line 1

thrust line 2

rn=aO (Drawing 4)   n

Drawing 3

thrust line 1

145. Drawing demonstrating the steps in making funicular polygon analysis of a barrel vault.

51

Drawing 2
(thrust line 1)

Drawing 4
(thrust line 2)

Drawing 5

Mb=46 m³
Fb= 744000N

tk=Fb
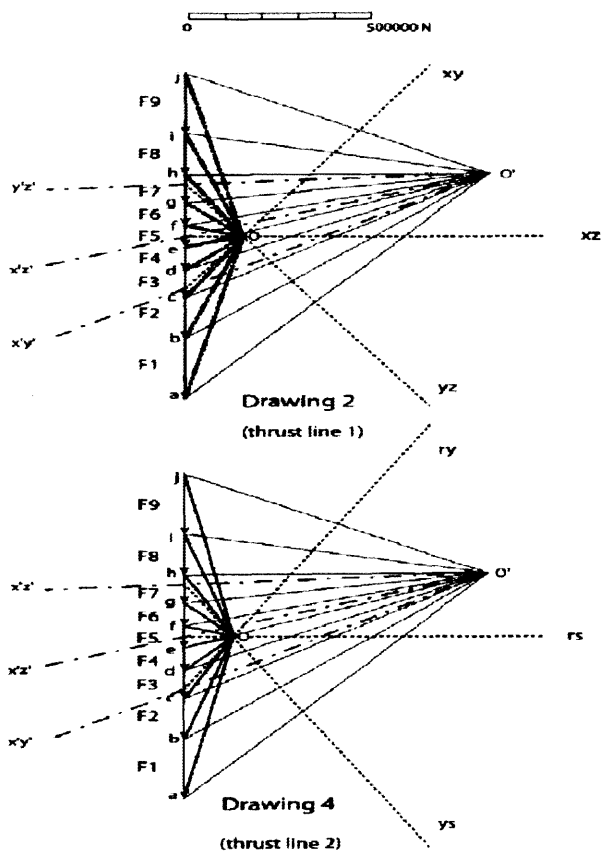
145 (continued)

F1 intersects the baseline at point x′, draw a line parallel to line bO′ (from Drawing 2) until it intersects the line of action of F2 (ignore line aO′ for now). At this point, draw the next line parallel to line cO′ until it intersects the line of action of F3. Continue until the diagram looks similar to Drawing 3. Then connect points x′, y′, and z′ to form a triangle x′y′z′. These points represent the intersections of the curve just drawn and the lines of action of the middle (F5) and the two outermost (F1, F9) force vectors.

6. Go back to Drawing 2 and draw lines parallel to lines x′y′, y′z′, and x′z′ (represented as single dash-dot lines on both Drawings 2 and 3) so that they pass through the trial pole O′.

7. Return to Drawing 1 and determine the three points (x, y, and z) through which the thrust curve should pass. All three points must be located on the line of action of one of the force vectors. To determine the minimum thrust (i.e., the steepest possible curve that will fit within the arch) for a barrel vault, one point (y) should be at the crown of the extrados. The other two points (x and z) should be on the lines of action of the outermost (F1, F9) force vectors. These locations can be estimated to get an idea of the path of the thrust line and then adjusted later. (In Drawing 1, I chose to start with the intersections at the impost of the vault.) Connect the three points with lines forming a triangle xyz. Ultimately, you want to define the curve that is tangent to the arch in three points. These are the three "hinges" of the three-hinge arch explained in Chapter 8.

8. Go to Drawing 2 and draw lines parallel to lines xy, yz, and xz from Drawing 1 (dotted lines) such that they pass through the intersections of the vertical line of vectors (aj) and the lines x′y′, x′z′, and y′z′. The intersection of the lines xy, yz, xz

provide the pole point O. The horizontal distance from O to the vertical line of vectors (aj) represents the horizontal thrust acting on the arch or vault.

9. On Drawing 2, draw lines connecting the pole point O to the ends of the vectors creating lines aO, bO, cO, and so on (thick dash–double dot lines).

10. The final step is to plot the line of thrust for the vault. On Drawing 3, draw a line parallel to line aO from Drawing 2 starting at point x′ (draw down and to the left). This is the vector representing the thrust on the abutment. Go back to point x′ and draw a line parallel to line bO from Drawing 2 until it intersects the line of action of F2. Then draw a line parallel to line cO until it intersects the line of action of F3. This process is a repeat of that in Step 5. The curve (thrust line 1) can then be transferred to Drawing 1 to see how it relates to the vault. (The curve can actually be drawn directly onto Drawing 1, but it is easier to see on Drawing 2.) If the final curve is not tangent to the intrados of the arch, points x and z must be moved up or down along their respective lines of action. Moving the points up will spread the curve out making it less steep, and moving them down will bring the curve in making it steeper. In the example illustrated, the curve needs to come in to touch the intrados, so the points are moved down. Connect the new points, r and s, so that they form triangle rys. Then repeat steps 8–10 as shown in Drawing 4 to create thrust line 2. Once the curve is tangent to the vault in three points, it is at the state of minimum thrust, which is the *limit state* indicating the point of stability because of the three hinges. This is a trial and error process and may take more than one try!

53

PART 2

PLOTTING THE LINE OF THRUST FROM THE VAULT DOWN THROUGH THE ABUTMENT: In the previous section, the minimum thrust of a stable three-hinged arch was established. The final part of determining the stability of the structure is to see whether the line of thrust remains within the thickness of the abutment. Because the drawing is symmetrical, the instructions are given only for the left abutment.

1. Calculate the mass (Mb) of the abutment and multiply it times the unit weight of the material used. Translate this weight into a force (Fb) into Newtons by multiplying by 9.8 m/sec/sec.

2. Determine the center of gravity of the abutment. For a rectangular abutment of the same material throughout, it will be located on the vertical centerline. This is the line of action of the force Fb.

3. At the intersection of line rn and the line of action of Fb, mark point t. Using the same scale used for the thrust line of the vault, draw a vector equal to Fb from t straight down along the line of action to k, such that tk = Fb. At point k, draw a line parallel and equal in length to line rn to create line ka. Finally, draw a line from t to a. This vector ta represents the magnitude and direction of the thrust on the abutment. If the line of action of vector ta remains within the thickness of the abutment, the structure is in equilibrium and will stand; however, a margin of safety is always desirable.

The process just described provides the steps involved in creating a funicular polygon diagram, but it does not explain the reasoning behind these steps. For further explanation of the funicular polygon method, see W. Zalewski and E. Allen, *Shaping Structures* (1998).

Appendix B – Sample Calculation and Results for Lateral Arch

Piece	Weight	A (top)		B (Top)		D (Bottom)		E (Bottom)		C (Centroid)	
	kN	x	y	x	y	x	y	x	y	x	y
Half	33.30	0.00	1.68	1.36	1.68	0.00	0.25	1.36	0.00	0.70	0.92
5	7.23	1.09	1.68	1.36	1.68	1.09	0.08	1.36	0.25	1.23	0.86
4	6.91	0.82	1.68	1.09	1.68	0.82	0.15	1.09	0.08	0.95	0.90
3	6.63	0.54	1.68	0.82	1.68	0.54	0.20	0.82	0.15	0.68	0.93
2	6.43	0.27	1.68	0.54	1.68	0.27	0.24	0.54	0.20	0.41	0.95
1	6.33	0.00	1.68	0.27	1.68	0.00	0.25	0.27	0.24	0.14	0.96

l	m	k	Hmin	d	d coord.		Vertical Reaction	
(m)	(m)	(m)	(kN)	(m)	x	y	Left	Right
1.36	0.70	1.68	13.10	0.00	0.00	1.68		
					1.36	0.00		
0.27	0.14	1.68	13.10	1.06	1.09	0.62	-26	33
0.27	0.14	1.06	13.10	0.59	0.82	1.09	-19	26
0.27	0.14	0.59	13.10	0.27	0.54	1.41	-13	19
0.27	0.14	0.27	13.10	0.07	0.27	1.61	-6	13
0.27	0.14	0.07	13.10	0.01	0.00	1.67	0	6

Appendix C – Sample Calculation and Results for Vault (Without Lateral Arch)

Piece	Weight kN	A (top) x	y	B (Top) x	y	D/G (Bottom) x	y	E (Bottom) x	y	C (Centroid) x	y
Half	866		6.32	5.8	6.32	0.99	0			2.02	3.97
1	304	0	6.32	1.16	6.32	0.99	0	1.16	0	0.58	3.16
2	263	1.16	6.32	2.32	6.32	1.16	0	2.32	2.4367	1.70	3.55
3	139	2.32	6.32	3.48	6.32	2.32	2.4367	3.48	4.0966	2.85	4.84
4	90	3.48	6.32	4.64	6.32	3.48	4.0966	4.64	4.7324	4.03	5.38
5	70	4.64	6.32	5.8	6.32	4.64	4.7324	5.8	4.92	5.21	5.59

l (m)	m (m)	d (m)	Hmin (kN)	k (m)	k coord. x	y	Vertical Reaction Left	Right
4.81	1.03		141.12				866.29	
					0.9867	0.00		
0.17	0.41	0.00	141.12	-0.19	1.16	-0.19	866	-562
1.16	0.54	-0.19	141.12	3.28	2.32	3.28	562	-299
1.16	0.53	0.84	141.12	2.67	3.48	5.11	299	-160
1.16	0.55	1.01	141.12	1.94	4.64	6.04	160	-70
1.16	0.57	1.30	141.12	1.59	5.80	6.32	70	0